A Hybrid Asymptotic-Numerical Method for Calculating Drag Coefficients in 2-D Low Reynolds Number Flows *

Sarah Hormozi, Michael J. Ward
Department of Mathematics, University of British Columbia, 1984 Mathematics Road, Vancouver, BC, V6T 1Z2, Canada.

March 3rd, 2014

Abstract. Steady state incompressible low Reynolds number fluid flow past a cylindrical body in an unbounded two-dimensional domain is a singular perturbation problem involving an infinite logarithmic expansion in the Reynolds number ε as $\varepsilon \to 0$. The central difficulty with applying a conventional matched asymptotic approach to this problem is that only the first few terms in the infinite logarithmic expansion of the drag coefficient and of the flow field can be calculated analytically. To overcome this difficulty, a hybrid asymptotic-numerical method that incorporates all logarithmic correction terms is implemented for three low Reynolds number flow problems. In particular, for a nanocylinder of circular cross-section with surface roughness, modeled by a Navier boundary condition involving a sliplength parameter, a hybrid asymptotic-numerical method is formulated and implemented to determine an approximation to the drag coefficient that is accurate to all powers of $-1/\log\varepsilon$. A similar analysis is done to determine a corresponding approximation of the drag coefficient for a porous cylinder, where the flow inside the cylinder is modeled by the Brinkman equation. For both the nano and porous cylinder problems, the hybrid asymptotic-numerical method is extended to calculate the first transcendentally small correction term to the Stokes flow near the body. This term, which governs weak upstream/downstream asymmetry in the Stokes flow, is extrapolated to finite ε to predict the formation of any eddies near the body. Finally, the hybrid method is used to determine the drag coefficient, valid to within all logarithmic terms, for two identical cylinders of circular cross-section in tandem alignment with the free stream. An extension of the theoretical framework to more general slow viscous flow problems is discussed.

Keywords: Logarithmic expansions, drag coefficient, singularity structure, nanocylinder, porous cylinder,

1. Introduction

In this paper we consider several variants of the classical problem of slow, steady, two-dimensional flow of a viscous incompressible fluid around an infinitely long straight cylinder of circular cross-section. By slow we mean that the Reynolds number $\varepsilon \equiv U_\infty L\rho_f/\mu$ is small, where ρ_f is the density of the fluid, U_∞ is the velocity of the fluid at infinity, μ is the dynamic viscosity, and L is the radius of the cross-section of the cylinder.

For a circular cylinder with no slip boundary condition, and in the limit $\varepsilon \to 0$, the method of matched asymptotic expansions was used systematically in [Kaplun (1957)] and in [Proudman & Pearson (1957)] to resolve the well-known Stokes paradox, and to calculate asymptotically the stream function in both the Stokes region, which is near the body, and in the Oseen region, which is far from the body. These pioneering studies showed that, for $\varepsilon \to 0$, the asymptotic expansion for the drag coefficient C_D of a circular cylindrical body starts with $C_D \sim 4\pi\varepsilon^{-1}\mathcal{F}(\varepsilon)$, where $\mathcal{F}(\varepsilon)$ is an infinite series in powers of $-1/\log\varepsilon$. The coefficients in this series are determined in terms of the solutions to certain forced Oseen problems.

In an effort to determine C_D quantitatively, analytical formulae for the first three coefficients in $\mathcal{F}(\varepsilon)$ were derived in [Kaplun (1957)]. However, as a result of the slow decay of $-1/\log\varepsilon$ with decreasing values of ε, the resulting three-term truncated series for C_D agrees rather poorly with the experimental results of [Tritton (1959)] unless ε is very small. Owing to the complexity of the calculations required, it is impractical to obtain a closer quantitative determination of the drag coefficient by calculating further coefficients in $\mathcal{F}(\varepsilon)$ analytically. As a result of these fundamental long-standing difficulties, the problem of slow viscous flow around a cylinder has served as a paradigm for problems where matched asymptotic analysis fails to be of much practical use, unless ε is very small. The development and application of singular perturbation methods to various problems in fluid mechanics is discussed in the classic text of [Van Dyke (1975)]. For a recent survey of the history of singular perturbations applied to boundary layer problems in fluid mechanics

* Email address for correspondence: ward@math.ubc.ca

see [O'Malley (2010)]. A comprehensive recent survey on asymptotic and renormalization group methods applied to slow viscous flow problems is given in [Veysey & Goldenfeld (2007)].

In [Kropinski *et al.* (1995)] a hybrid asymptotic-numerical method was formulated and implemented to effectively sum the infinite logarithmic expansions that arise from the singular perturbation analysis of slow viscous flow around a cylinder that has a cross-section that is symmetric with respect to the free stream. This approach differed from the hybrid method employed in [Lee & Leal (1986)] in which numerical methods are used within the framework of the method of matched asymptotic expansions to calculate the first few coefficients in the logarithmic expansions of the flow field and the drag coefficient. Instead, it was shown in [Kropinski *et al.* (1995)] that the entire infinite logarithmic series is contained in the solution to a certain related problem that does not involve the cross-sectional shape of the cylinder. The methodology of [Kropinski *et al.* (1995)] to treat infinite logarithmic expansions was extended in [Titcombe *et al.* (2000)] to allow for cylinders of arbitrary cross-section that are not necessarily symmetric with respect to the free stream.

In two dimensional domains, infinite logarithmic expansions also arise in the analysis of singularly perturbed eigenvalue problems (cf. [Ward *et al.* (1993)], [Kolokolnikov *et al.* (2005)]), in calculating the mean first passage time for a Brownian particle to leave a domain through a narrow gap (cf. [Pillay *et al.* (2010)]), in nonlinear biharmonic problems of MEMS (cf. [Kropinski *et al.* (2011)]), and in the analysis of localized spot patterns for reaction diffusion systems (cf. [Chen & Ward (2011)]). A unified theoretical framework to treat such diverse problems with infinite logarithmic series is surveyed in [Ward & Kropinski (2010)].

The main goal of this paper is to extend this previous theoretical framework to study two different low Reynolds number flows past a cylindrical body of circular cross-section. In §4 we consider slow viscous flow past a nanocylinder of circular cross-section that has boundary surface roughness. This surface roughness is modeled by a Navier boundary condition involving a dimensionless sliplength parameter. In §5 we study slow viscous flow past a porous cylinder, where the fluid inside the cylinder is modeled by the Brinkman equation. For the nanocylinder problem for a given sliplength, [Matthews & Hill (2006)] derived an explicit three-term approximation to the infinite logarithmic series for the drag coefficient. A similar low-order truncated series result for the drag coefficient of a porous cylinder at a fixed Darcy number was derived in [Kohr *et al.* (2009)]. For these two problems we formulate a hybrid asymptotic-numerical method to calculate an approximation $C_D^\star$ for the drag coefficient that is accurate to all powers of $-1/\log\varepsilon$. Our analysis show that $C_D^\star$ is given by

$$C_D^\star = 4\pi\varepsilon^{-1}S(\nu)\,, \tag{1.1}$$

where $S(\nu)$ satisfies a nonlinear algebraic equation of the form

$$\frac{S}{R(S)} = \nu \equiv -\frac{1}{\log(\varepsilon e^c)}\,. \tag{1.2}$$

In (1.2), the constant c is determined by the Stokes streamfunction solution ψ_c near the body, which has the asymptotic behavior $\psi_c \sim r\log r\,\sin\theta$ as $r\to\infty$, where r is the distance from the center of the cross-section of the cylinder. The constant c is identified from the next term in the far-field behavior of ψ_c given by

$$\psi_c \sim (r\log r - cr + o(1))\sin\theta\,, \qquad \text{as} \quad r\to\infty\,. \tag{1.3}$$

For the nanocylinder with surface roughness or the porous cylinder, the constant c can be calculated in terms of the sliplength or the Darcy number, respectively. In contrast, in (1.2) the nonlinear function $R(S)$, with $R(0)=1$, is calculated from the streamfunction solution $\Psi_H(\rho,\theta)$, with $\rho=\varepsilon r$, associated with the full Navier-Stokes equation. This streamfunction satisfies a nonlinear biharmonic problem subject to the free stream condition $\Psi_H\sim\rho\sin\theta$ as $\rho\to\infty$, and a parameter-dependent singularity condition $\Psi_H\sim S\rho\log\rho\sin\theta$ as $\rho\to 0$. In terms of the solution Ψ_H, the nonlinear function $R(S)$ is identified from the next order term in the local behavior of Ψ_H as $\rho\to 0$ given by

$$\Psi_H \sim S\rho\log\rho\sin\theta + R(S)\rho\sin\theta\,, \quad \text{as} \quad \rho\to 0\,. \tag{1.4}$$

Since $R(S)$ is independent of the any details of the Stokes solution near the body, this "universal" function can be accurately pre-computed numerically and then used for both the nano and porous cylinder problems.

We remark that $c = 1/2$ for the classical problem of an impermeable cylinder with circular cross-section with no boundary slip. It follows from (1.2) that once c is identified from the appropriate Stokes solution near the body for either of the problems in §4 or §5, the corresponding drag coefficient will be the same to within all logarithmic terms as that of this classical problem at the new Reynolds number $\varepsilon_{\text{class}} = \varepsilon e^{c-1/2}$. This observation is a simply another manifestation of the well-known Kaplun's equivalence principle [Kaplun (1957)]. In its original form this principle states that, corresponding to every cylinder of arbitrary cross-section which is symmetric with respect to the free stream, there exists an equivalent cylinder of circular cross-section of a certain radius that has the same drag coefficient to within all logarithmic correction terms. Therefore, our theoretical framework for determining C_D can be viewed as a hybrid asymptotic-numerical method of implementing a related equivalence principle for the nano and porous cylinder problems.

In addition to calculating the drag coefficient, in §4 and §5 we show how to calculate the first transcendentally small in ε term in the Stokes flow field near the body. The calculation of this term, which involves a further "universal" function $\mathcal{C}_2(S)$ obtained from a more refined local behavior of Ψ_H than given in (1.4), determines any weak upstream/downstream asymmetry in the flow field near the body. However, it does not contribute to any transcendentally small correction term to the determination of the drag coefficient. In §4 we evaluate this term at finite ε as a way to predict how the formation of an eddy near the body depends on the sliplength parameter and the Reynolds number. This analysis of deriving and then utilizing the first transcendentally small correction term in the Stokes region to predict eddy formation is an extension of that in [Keller & Ward (1996)] where the corresponding problem with no boundary slip was investigated.

In §2 we give a brief outline of the conventional singular perturbation analysis of [Kaplun (1957)] and [Proudman & Pearson (1957)] for determining the drag coefficient, and we summarize the hybrid asymptotic-numerical framework of [Kropinski *et al.* (1995)] for effectively calculating all the logarithmic terms in the expansion of C_D. We then give a new result characterizing a refined local approximation for Ψ_H as $\rho \to 0$, which allows for the identification of the "universal" functions $R(S)$ and $\mathcal{C}_2(S)$. Numerical results for these quantities are given and their best fit approximations to low degree polynomials in S are obtained.

In §3 we introduce a new simple model problem that is used to illustrate the hybrid asymptotic-numerical method for effectively "summing" infinite logarithmic series for singularly perturbed biharmonic problems. Conventionally, the singular perturbation problem for $u(r)$ given by $u'' + r^{-1}u' + uu' = 0$ on $\varepsilon < r < \infty$ with $u(\varepsilon) = 0$ and $u \to 1$ as $r \to \infty$ has been used as a crude model of low Reynolds number flow and to illustrate the difficulty with treating logarithmic expansions (cf. [Hinch (1991)], [Lagerstrom (1988)], [Veysey & Goldenfeld (2007)]). Our introduction and analysis of the model biharmonic problem in §3 provides an alternative to this classical model problem. By calculating both an exact solution and a term-by-term infinite series approximate solution to our new model problem, we show clearly how the hybrid method is able to capture all of the logarithmic terms in the expansion of the solution.

In §6 we briefly re-consider the classical problem of slow viscous flow past two identical cylinders of circular cross-section, with no boundary slip, that are aligned in tandem with the free-stream. A more general problem, with no assumed symmetry of the cylinder cross-sections with the flow field, was considered in [Umemura (1982)] and [Lee & Leal (1986)], where the first few logarithmic terms in the asymptotic expansion of the drag coefficient were calculated. In [Dorrepaal §O'Neil (1979)] and [Miyazaki & Hasimoto (1980)], the leading-order Stokes solution was shown to produce a rather intricate eddy structure between two cylinders in tandem alignment with the free-stream when the distance between the cylinders is varied. In §6 we extend this previous work by using our hybrid asymptotic-numerical method to calculate the approximation $C_D^\star$ in (1.1) to the drag coefficient for two tandem identical cylinders. For this problem, the parameter c in (1.2) is calculated as a function of the distance between the centers of the cross-sections of the cylinders by adapting the approach of [Umemura (1982)] where a bipolar coordinate transformation was used to calculate the Stokes streamfunction. Since the leading-order Stokes solution already has a

well-known eddy structure depending on the inter-cylinder distance (cf. [Dorrepaal §O'Neil (1979)] and [Miyazaki & Hasimoto (1980)]), we do not see the need to extend the hybrid method to calculate the first transcendentally small term in the Stokes region for the two-cylinder problem.

Finally, in §7 we list a few open problems and we outline how our theoretical framework for treating infinite logarithmic expansions in low Reynolds number flow problems can be extended to more general problems involving bodies of arbitrary cross-section where there is no symmetry with respect to the free stream.

2. The Hybrid Formulation

We first outline the conventional singular perturbation analysis of (2.1)–(2.3) for $\varepsilon \to 0$ (cf. [Kaplun (1957)] and [Proudman & Pearson (1957)]) for slow, steady, incompressible, viscous flow around a circular cylindrical body with a uniform stream of speed U_∞ in the x direction at large distances from the body. We then formulate the hybrid method of [Kropinski *et al.* (1995)] for summing the infinite-order logarithmic expansions that arise from the analysis.

In terms of polar coordinates centred inside the body, it is well-known that the dimensionless stream function ψ satisfies

$$\Delta_r^2\psi \;=\; -\varepsilon\, J_r\left[\psi, \Delta_r\psi\right]\,, \quad \text{for} \quad r>1\,, \tag{2.1}$$

$$\psi \;=\; \partial_r\psi = 0\,, \quad \text{on} \quad r=1\,, \tag{2.2}$$

$$\psi \;\sim\; r\sin\theta\,, \quad \text{as} \quad r\to\infty\,. \tag{2.3}$$

Here $\varepsilon \equiv U_\infty L\rho_f/\mu \ll 1$ is the Reynolds number based on the radius L of the cylinder, μ is the dynamic viscosity, ρ_f is the fluid density, Δ_r and Δ_r^2 denote the Laplacian and biharmonic operators in terms of the Stokes variable r, respectively, and $J_r\left[a,b\right] \equiv r^{-1}\left(\partial_r a\,\partial_\theta b - \partial_\theta a\,\partial_r b\right)$ is the Jacobian.

In the Stokes, or inner, region where $r=\mathcal{O}(1)$, the stream function has an infinite logarithmic expansion, referred to as the Stokes expansion, of the form

$$\psi_s(r,\theta) = \sum_{j=1}^{\infty} \nu^j \psi_j(r,\theta) + \cdots\,, \tag{2.4}$$

where $\nu = \nu(\varepsilon) \equiv -1/\log\left(\varepsilon e^{1/2}\right)$. Upon substituting (2.4) into (2.1), we obtain that $\psi_j = a_j\psi_c$, where the a_j for $j\geq 1$ are undetermined constants and $\psi_c \equiv \psi_c(r,\theta)$ is the unique solution to the canonical Stokes problem

$$\Delta_r^2\psi_c \;=\; 0\,, \quad \text{for} \quad r>1\,, \tag{2.5}$$

$$\psi_c \;=\; \psi_{cr} = 0\,, \quad \text{on} \quad r=1\,, \tag{2.6}$$

$$\psi_c \;\sim\; r\log r\sin\theta\,, \quad \text{as} \quad r\to\infty\,, \tag{2.7}$$

which has the solution

$$\psi_c = \left(r\log r - \frac{r}{2} + \frac{1}{2r}\right)\sin\theta\,. \tag{2.8}$$

Upon substituting $\psi_j = a_j\psi_c$ and (2.8) into (2.4), the far-field behaviour of the Stokes expansion is

$$\psi_s(r,\theta) \sim \sum_{j=1}^{\infty} \nu^j\, a_j \left(\log r - \log\left[e^{1/2}\right]\right) r\sin\theta\,, \quad \text{as} \quad r\to\infty\,. \tag{2.9}$$

In terms of the Oseen, or outer, length-scale ρ, defined by $\rho = \varepsilon r$, (2.9) becomes

$$\psi_s \sim \frac{1}{\varepsilon}\left(a_1\rho\sin\theta + \sum_{j=1}^{\infty}\nu^j\,\left[a_j\rho\log\rho + a_{j+1}\rho\right]\sin\theta\right)\,. \tag{2.10}$$

This expression provides a singularity structure for the Oseen, or outer, solution as $\rho \to 0$.

The behaviour (2.10) suggests that in the Oseen region, where $\rho = \mathcal{O}(1)$, we introduce the new variable Ψ by $\Psi(\rho,\theta) = \varepsilon\psi(\varepsilon^{-1}\rho,\theta)$, and that we expand Ψ as

$$\Psi(\rho,\theta) = \rho\sin\theta + \nu\Psi_1(\rho,\theta) + \sum_{j=2}^{\infty}\nu^j\Psi_j(\rho,\theta) + \cdots\,, \tag{2.11}$$

in order to satisfy the free-stream condition as $\rho \to \infty$ in (2.3). Upon substituting (2.11) into (2.1), and matching Ψ as $\rho \to 0$ to the required singular behaviour (2.10), we find that $a_1 = 1$ and that Ψ_j, for $j \geq 1$, satisfy the following forced Oseen problems on $0 < \rho < \infty$:

$$L_{0s}\Psi_1 \;\equiv\; \Delta_\rho^2\Psi_1 + \left(\rho^{-1}\sin\theta\,\partial_\theta - \cos\theta\,\partial_\rho\right)\,\Delta_\rho\Psi_1 = 0\,, \tag{2.12}$$

$$\Psi_1 \;\sim\; (\log\rho + a_2)\,\rho\sin\theta\,, \quad \text{as} \quad \rho\to 0\,; \quad \partial_\rho\Psi_1 \to 0\,, \quad \text{as} \quad \rho\to\infty\,, \tag{2.13}$$

$$L_{0s}\Psi_j \;=\; -\sum_{k=1}^{j-1} J_\rho\left[\Psi_k, \Delta_\rho\Psi_{j-k}\right]\,, \tag{2.14}$$

$$\Psi_j \;\sim\; (a_j\log\rho + a_{j+1})\,\rho\sin\theta\,, \quad \text{as} \quad \rho\to 0\,; \quad \partial_\rho\Psi_j \to 0\,, \quad \text{as} \quad \rho\to\infty\,. \tag{2.15}$$

Here L_{0s} is the linearized Oseen operator and Ψ_1 is the linearized Oseen solution.

The forced Oseen problems in (2.12)–(2.15) recursively determine the coefficients a_j for $j \geq 2$. The first two coefficients are well-known, and are given by (cf. [Kaplun (1957)], [Proudman & Pearson (1957)])

$$a_2 \;=\; \gamma_e - \log 4 - 1 \approx -1.8091\,, \tag{2.16}$$

$$a_3 - a_2^2 \;=\; -\int_0^\infty \left[r^{-1}I_1(2r) + 1 - 4K_1(r)I_1(r)\right]K_0(r)K_1(r)\,dr \approx -0.8669\,. \tag{2.17}$$

Here K_1, K_0, I_0 and I_1 are the usual modified Bessel functions, and γ_e is Euler's constant. The expression for a_2 was first obtained in [Proudman & Pearson (1957)], while the expression for a_3 was given in [Kaplun (1957)]. Explicit analytical formulae for a_j when $j \geq 4$ are not available.

In terms of the constants a_j for $j \geq 2$, the well-known drag coefficient C_D is given by (cf. [Kaplun (1957)])

$$C_D \sim 4\pi\varepsilon^{-1}\nu\left(1 + \sum_{j=2}^{\infty} a_j\nu^{j-1} + \cdots\right)\,, \qquad \nu \equiv -\frac{1}{\log\left[\varepsilon e^{1/2}\right]}\,. \tag{2.18}$$

However, as discussed in [Van Dyke (1975)] (see also [Veysey & Goldenfeld (2007)]), the truncated three-term expansion for C_D agrees rather poorly with the experimentally measured drag coefficient of [Tritton (1959)] unless ε is very small (cf. [Van Dyke (1975)]).

In order to obtain a higher order approximation to the drag coefficient than afforded by the coefficients a_2 and a_3, one can, in principle, compute numerically further coefficients a_j, for $j \geq 4$, from the the infinite sequence of PDE's (2.14) with singularity structures (2.15). This recursive determination of the coefficients would still require truncating the series (2.18) at some finite j. As an alternative to series truncation, in [Kropinski *et al.* (1995)] a hybrid asymptotic-numerical method was proposed that has the effect of summing all the terms on the right-hand side of (2.18), but which avoids computing the coefficients a_j for $j \geq 1$ individually.

In this hybrid approach of [Kropinski *et al.* (1995)], the Oseen solution is no longer expanded in powers of ν as in (2.11). Instead, the full problem (2.1)–(2.3) for $\rho > 0$ is solved subject to a parameter-dependent singularity structure, which is to hold as $\rho \to 0$. In this way, $\Psi_H \equiv \Psi_H(\rho,\theta;S)$ is defined to be the solution to

$$\Delta_\rho^2\Psi_H \;=\; -J_\rho\left[\Psi_H, \Delta_\rho\Psi_H\right]\,, \quad \rho > 0\,, \tag{2.19}$$

$$\Psi_H \;\sim\; \rho\sin\theta\,, \quad \text{as} \quad \rho\to\infty\,, \tag{2.20}$$

$$\Psi_H \;\sim\; S\rho\log\rho\sin\theta\,, \quad \text{as} \quad \rho\to 0\,. \tag{2.21}$$

In [Kropinski *et al.* (1995)], this parameter-dependent problem is solved numerically for a range of S values, and in terms of this solution we identify the regular part $R = R(S)$ of the singularity structure at the origin by the limiting process

$$\Psi_H - S\rho\log\rho\sin\theta = R(S)\rho\sin\theta + o(\rho)\,, \quad \text{as} \quad \rho\to 0\,. \tag{2.22}$$

Upon introducing the Stokes variables r and ψ defined by $r = \rho/\varepsilon$ and $\psi = \psi_H/\varepsilon$, (2.22) becomes

$$\psi \sim \left[Sr\log r + (S\log\varepsilon + R)\, r\right]\sin\theta\,, \tag{2.23}$$

which determines the required far-field behaviour of the Stokes solution. The Stokes, or inner, solution that satisfies $\psi \sim Sr\log r\sin\theta$ as $r\to\infty$ is simply $\psi = S\psi_c$, where ψ_c is given in (2.8). Finally, upon matching the $\mathcal{O}(r\sin\theta)$ terms in (2.23) and $S\psi_c$, we obtain that $S = S(\nu)$ satisfies the transcendental equation

$$\frac{S}{R(S)} = \nu \equiv -\frac{1}{\log\left[\varepsilon e^{1/2}\right]}\,. \tag{2.24}$$

In terms of $S = S(\nu)$, the drag coefficient accurate to all powers of ν is (see Appendix A)

$$C_D \sim 4\pi\varepsilon^{-1}S(\nu) = 4\pi\varepsilon^{-1}\nu R\left[S(\nu)\right]\,. \tag{2.25}$$

This completes the summary of the hybrid method of [Kropinski *et al.* (1995)].

In the next section, we need the following higher order result for the local behaviour of ψ_H as $\rho\to 0$:

LEMMA 1. *The solution to (2.19)–(2.22) has the following asymptotic behaviour as $\rho\to 0$:*

$$\begin{aligned}\Psi_H \;\sim\; &\left[S\rho\log\rho + R\rho + o(\rho)\right]\sin\theta \\ &+ \left[\frac{S^2}{16}\left(\rho\log\rho\right)^2 + \frac{1}{8}\left(SR + \frac{S^2}{4}\right)\rho^2\log\rho + \mathcal{C}_2\rho^2 + o(\rho^2)\right]\sin(2\theta) + \cdots\,.\end{aligned} \tag{2.26}$$

Here $R = R(S)$ and $\mathcal{C}_2 = \mathcal{C}_2(S)$ must be computed from (2.19)–(2.22). To leading order as $S\to 0$, we have

$$R = 1 + a_2 S + \mathcal{O}(S^2)\,, \qquad \mathcal{C}_2 = \frac{S}{8}\left(a_2 + \frac{1}{2}\right) + \mathcal{O}(S^2)\,, \tag{2.27}$$

where a_2 is defined in (2.16). At one higher order, the curve $R = R(S)$ for $S\to 0$ is given parametrically in terms of $\delta \ll 1$ by

$$S = \delta + a_2\delta^2 + \cdots\,, \qquad R \sim 1 + a_2\delta + a_3\delta^2 + \cdots\,, \tag{2.28}$$

where a_3 is defined in (2.17). This yields the three-term approximation for $R(S)$

$$R(S) \sim 1 + a_2 S + \left(a_3 - a_2^2\right)S^2 + \mathcal{O}(S^3)\,, \quad \textit{for} \quad S \ll 1\,. \tag{2.29}$$

Proof: To derive (2.26) regarding higher order terms for Ψ_H as $\rho\to 0$ we let $\Psi_H = (S\log\rho + R)\,\rho\sin\theta + \tilde{\Psi}$, where $\tilde{\Psi} \ll 1$, to obtain from (2.19) that

$$\Delta_\rho^2\tilde{\Psi} \sim -J_\rho\left(\Psi_H, \Delta_\rho\Psi_H\right) \sim -\left[2S^2\log\rho + \left(S^2 + 2RS\right)\right]\frac{\sin(2\theta)}{\rho^2}\,. \tag{2.30}$$

We write $\tilde{\Psi}(\rho,\theta) = e^{2t}f(t)\sin(2\theta)$, where $t = \log\rho$, to conclude that $f(t)$ satisfies

$$f'''' + 4f''' - 4f'' - 16f' = -2S^2 t - \left(S^2 + 2RS\right)\,. \tag{2.31}$$

The particular solution is readily found and the homogeneous solution is a linear combination of the elementary functions $\{1, e^{-2t}, e^{2t}, e^{-4t}\}$. Therefore,

$$f(t) = \frac{S^2t^2}{16} + \frac{t}{8}\left(RS + \frac{S^2}{4}\right) + \mathcal{C}_0 e^{-4t} + \mathcal{C}_1 e^{-2t} + \mathcal{C}_2 + \mathcal{C}_3 e^{2t}\,, \tag{2.32}$$

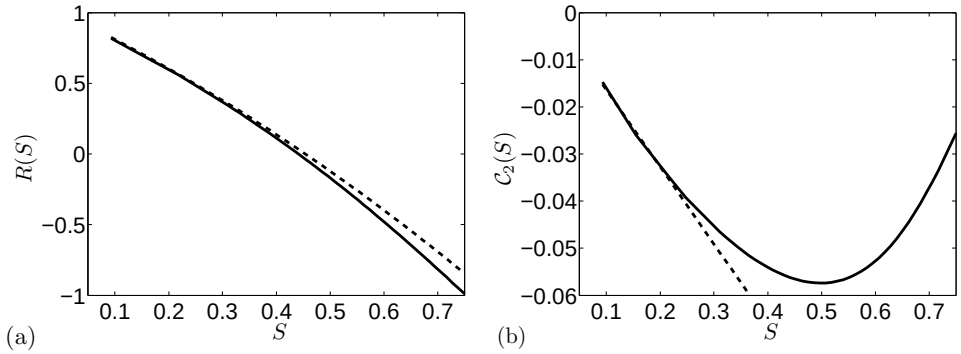

Figure 1. (a) Plot of $R = R(S)$ computed numerically from the hybrid formulation (2.19)–(2.22) (solid curve). The curve $R(S) = 0.9976 - 1.8930S - 0.264S^2 - 1.7131S^3 + 0.9578S^4$ is the best least squares quartic polynomial to the numerical data for $R(S)$. The three-term approximation (2.29) is the dashed curve. (b) Plot of $\mathcal{C}_2 = \mathcal{C}_2(S)$ computed numerically from the hybrid formulation (2.19)–(2.22) (solid curve). The curve $\mathcal{C}_2(S) = 0.0087 - 0.3131S + 0.8171S^2 - 1.8982S^3 + 2.4997S^4 - 1.0492S^5$ is the best quintic polynomial to the numerical data for $\mathcal{C}_2(S)$. The one-term approximation (2.27) is the dashed curve, which provides a rather poor approximation unless S is rather small.

where we must set $\mathcal{C}_3 = 0$ to eliminate exponential growth in f. Upon using (2.32), and recalling $\tilde{\Psi}(\rho,\theta) = e^{2t} f(t)\sin(2\theta)$ where $t = \log\rho$, we obtain (2.26).

Next, the result (2.28) for S and $R(S)$ as $S \to 0$ follows immediately from the expansion (2.11) and the singularity behaviours in (2.13) and in (2.15) for $j = 2$. Reversion of series then yields (2.29). Finally, to establish (2.27) for $\mathcal{C}_2(S)$ as $S \to 0$, we need only determine the behaviour as $\rho \to 0$ of the linearized Oseen solution Ψ_1 satisfying (2.12) and (2.13). This solution is given by (cf. [Proudman & Pearson (1957)])

$$\Psi_1 = -\sum_{n=1}^{\infty} \frac{\beta_n(\rho/2)}{n}\rho\sin(n\theta)\,, \qquad \beta_n(\xi) \equiv 2\left[K_1(\xi)I_n(\xi) + K_0(\xi)I_n'(\xi)\right]\,, \tag{2.33}$$

where K_0, K_1, I_n, and I_n' are the usual Bessel functions. In the limit $\rho \to 0$, we readily calculate that

$$\Psi_1 \sim (\rho\log\rho + a_2\rho + o(\rho))\sin\theta + \left[\frac{\rho^2}{8}\left(a_2 + \frac{1}{2}\right) + \frac{\rho^2}{8}\log\rho + o(\rho^2)\right]\sin(2\theta) + \cdots\,. \tag{2.34}$$

Since for $S \ll 1$, we have $\Psi_H \sim \rho\sin\theta + S\Psi_1 + \mathcal{O}(S^2)$, it follows that the $\mathcal{O}(\rho^2)$ term in (2.34) must be $\mathcal{C}_2/S$, where $\mathcal{C}_2$ is defined in (2.26). This establishes (2.27) for $\mathcal{C}_2$, and completes the proof of Lemma 1. ■

A plot of the numerically computed function $R = R(S)$, together with its three-term approximation from (2.29), is shown in Fig. 1(a). In Fig. 1(b) we also plot the numerically computed $\mathcal{C}_2(S)$ versus S and compare it with its leading-order approximation from (2.27). In the caption of this figure, the numerical results for $R(S)$ and $\mathcal{C}_2(S)$ are then accurately fit in a least squares sense to low degree polynomials in S.

The numerical method used to calculate $R(S)$ and $\mathcal{C}_s(S)$ from the solution Ψ_H to (2.19)–(2.22) is described in Appendix A of [Keller & Ward (1996)] (see also §4.2 of [Kropinski *et al.* (1995)]). We only briefly outline it here. The numerical approach is based on first decomposing Ψ_H as $\Psi_H = \rho\sin\theta + S\Psi_1 + \Psi_H^\star$ where Ψ_1 is the linearized Oseen solution in (2.33). This solution has the correct singularity $S\Psi_1 \sim S\rho\log\rho\sin\theta$ as $\rho \to 0$ and has the far-field behavior $\Psi_1 \to 0$ as $\rho \to \infty$. Upon substituting this decomposition for Ψ_H into (2.19)–(2.22), we obtain that $\Psi_H^\star(\rho,\theta;S)$ is C^1 as $\rho \to 0$ and satisfies the nonlinear problem

$$\begin{aligned} L_{0s}\Psi_H^\star &= -J_\rho\left[S\Psi_1 + \Psi_H^\star, S\Delta\Psi_1 + \Delta_\rho\Psi_H^\star\right]\,, \quad \rho > 0\,, \quad 0 < \theta < \pi\,, \\ \partial_\rho\Psi_H^\star &\to 0\,, \quad \text{as} \quad \rho \to \infty\,; \qquad \Psi_H^\star(\rho,\theta) = -\Psi_H^\star(\rho,-\theta)\,, \end{aligned}$$

where L_{0s} is the linearized Oseen operator. As $\rho \to 0$, $\Psi_H^\star$ has the following local behavior in terms of Fourier sine coefficients:

$$\Psi_H^\star \sim \Psi_{H1}^\star(\rho;S)\sin\theta + \Psi_{H2}^\star(\rho;S)\sin(2\theta) + \cdots; \quad \Psi_{Hj}^\star(\rho;S) \equiv \frac{2}{\pi}\int_0^\pi \Psi_H^\star(\rho,\theta;S)\sin(j\theta)\,d\theta\,, \;\; j=1,2\,. \tag{2.35}$$

The function $\Psi_H^\star$ is computed with a finite difference method (see §4.2 of [Kropinski *et al.* (1995)]) and the Fourier sine coefficients $\Psi_{Hj}^\star$ for $\rho \ll 1$ are evaluated by a numerical quadrature (cf. Appendix A of [Keller & Ward (1996)]).

To compute $R = R(S)$, we simply equate for $\rho \ll 1$ the coefficients of $\sin\theta$ in our decomposition of Ψ_H with that of the required behavior for Ψ_H given in (2.22). This yields $S\rho\log\rho + R\rho \sim \rho - S\rho\beta_1(\rho/2) + \Psi_H^\star(\rho;S)$ as $\rho \to 0$. Then, since $\beta_1(\rho/2) \sim 1 - \log\rho + \log 4 - \gamma$ as $\rho \to 0$, where γ is Euler's constant, we obtain that $R = R(S)$ is given by

$$R = 1 - S(1 + \log 4 - \gamma) + \lim_{\rho\to 0}\frac{\Psi_H^\star(\rho;S)}{\rho}\,. \tag{2.36}$$

In a similar way, by equating the coefficients of $\sin(2\theta)$ as $\rho \to 0$ between our decomposition of Ψ_H and the required behavior in (2.26) we can identify and then compute $\mathcal{C}_2(S)$. Further details of the method are given in §4.2 of [Kropinski *et al.* (1995)] and Appendix A of [Keller & Ward (1996)].

3. An Exactly Solvable Model Problem

In this section we illustrate the approach for treating biharmonic problems with infinite logarithmic expansions by considering the following simple singularly perturbed problem in an annulus:

$$\Delta_\rho^2 u = 0\,, \quad \varepsilon < \rho < 1\,, \tag{3.1}$$

$$u = \sin\theta\,, \quad u_\rho = 0\,, \quad \text{on} \quad \rho = 1\,, \tag{3.2}$$

$$u = u_\rho = 0\,, \quad \text{on} \quad \rho = \varepsilon\,. \tag{3.3}$$

We first perform a direct infinite order logarithmic expansion of the solution to (3.1)–(3.3) for $\varepsilon \to 0$ by using the method of matched asymptotic expansions. To leading order in the outer region where $\rho \gg \mathcal{O}(\varepsilon)$, we obtain that $u \sim u_0$, where u_0 is smooth as $\rho \to 0$ and satisfies $\Delta_\rho^2 u_0 = 0$ in $0 < \rho < 1$ with $u_0 = \sin\theta$ and $u_{0\rho} = 0$ on $\rho = 1$. The solution is

$$u_0 = \left(\frac{3\rho}{2} - \frac{\rho^3}{2}\right)\sin\theta\,. \tag{3.4}$$

In terms of the inner variable $r = \rho/\varepsilon$, we obtain the matching condition for the inner solution that

$$u \sim u_0 \sim \frac{3\varepsilon}{2} r\sin\theta + \mathcal{O}(\varepsilon^3)\,. \tag{3.5}$$

Now if in the inner region we pose $u = \varepsilon\tilde{U}$, then we would conclude that $\Delta_r^2\tilde{U} = 0$ in $r \geq 1$ with $\tilde{U} = \tilde{U}_r = 0$ on $r = 1$ and with $\tilde{U} \sim (3r/2)\sin\theta$ as $r \to \infty$, as obtained from the matching condition (3.5). However, it is readily verified that there is no solution to this problem. This is another manifestation of the Stokes paradox (cf. [Proudman & Pearson (1957)]). Instead we must insert a logarithmic scale ν of order $\mathcal{O}(-1/\log\varepsilon)$ to be found and pose $u = \varepsilon\nu\tilde{U}_0$ in the inner region where $\tilde{U}_0 \sim \mathcal{O}(r\log r\sin\theta)$ as $r \to \infty$. More specifically, our leading-order inner solution is

$$u \sim \varepsilon\nu B_0\psi_c\,, \tag{3.6}$$

where B_0 is an undetermined constant, and where $\psi_c(r,\theta)$ is the solution to the canonical Stokes problem (2.5)–(2.6) given in (2.8). Upon writing the far-field behavior of ψ_c in terms of the outer variable $\rho = \varepsilon r$, we readily obtain that

$$u \sim B_0 \rho \sin\theta + \nu B_0 \rho \log\rho \, \sin\theta + \mathcal{O}(\varepsilon^2 \nu)\,, \qquad \text{where} \qquad \nu \equiv -1/\log(\varepsilon e^{1/2})\,. \tag{3.7}$$

By asymptotically matching this expression with (3.4) when $\rho \ll 1$, we conclude that $B_0 = 3/2$ and that we must add a term of order $\mathcal{O}(\nu)$ in the outer region.

To proceed to higher order in powers of ν, we pose an infinite order logarithmic expansion in the inner region of the form

$$u = \varepsilon\nu \left(B_0 + B_1\nu + B_2\nu^2 + \cdots\right)\psi_c\,, \tag{3.8}$$

where $\psi_c(r,\theta)$ is given in (2.8). Upon writing the far-field behavior of this inner expansion in terms of the outer variable $\rho = \varepsilon r$, we obtain the matching condition

$$u = B_0\rho\sin\theta + \sum_{j=1}^{\infty} \nu^j \left[B_j + B_{j-1}\log\rho\right]\rho\sin\theta + \mathcal{O}(\varepsilon^2\nu)\,, \quad \text{as} \quad \rho \to 0\,, \tag{3.9}$$

for the solution to the outer problem. Therefore, in the outer region, the outer expansion must have the form

$$u = u_0 + \sum_{j=1}^{\infty} \nu^j u_j + \cdots\,, \tag{3.10}$$

where u_0 is given in (3.4). Upon substituting this expansion into (3.1) and (3.2), and by noting the matching condition (3.9), we obtain that u_j for $j \geq 1$ satisfies

$$\Delta_\rho^2 u_j = 0\,, \quad 0 < \rho < 1\,; \quad u_j = u_{j\rho} = 0\,, \quad \text{on} \quad \rho = 1\,, \tag{3.11}$$

with $u_j \sim B_{j-1}\rho\log\rho\sin\theta$ as $\rho \to 0$. The unique solution to this problem is

$$u_j = \left(B_{j-1}\rho\log\rho + \frac{B_{j-1}}{2}(\rho - \rho^3)\right)\sin\theta\,. \tag{3.12}$$

Then, from (3.9), the constant B_j is identified from the matching condition requirement that $u_j \sim (B_{j-1}\rho\log\rho + B_j\rho)\sin\theta$ as $\rho \to 0$. Therefore, we conclude from (3.12) that the coefficients B_j for $j \geq 0$ in (3.8) satisfy the recursion relation

$$B_j = \frac{1}{2}B_{j-1}\,, \quad j \geq 1\,; \qquad B_0 = \frac{3}{2}\,. \tag{3.13}$$

This shows that the infinite order logarithmic expansions are in fact convergent geometric series. Finally, by summing these infinite order logarithmic expansions, we obtain for the inner region that

$$u \sim \nu \sum_{j=0}^{\infty} B_j \nu^j \psi_c = B\psi_c\,, \qquad B = B(\nu) \equiv \frac{3\nu}{2-\nu}\,, \tag{3.14}$$

and for the outer region that

$$u \sim \left(\frac{3\rho}{2} - \frac{\rho^3}{2}\right)\sin\theta + \sum_{j=1}^{\infty} \nu^j B_{j-1}\left(\rho\log\rho + \frac{\rho}{2} - \frac{\rho^3}{2}\right)\sin\theta = \left(B\rho\log\rho + \frac{B}{\nu}\rho - \frac{1}{2}(1+B)\rho^3\right)\sin\theta\,. \tag{3.15}$$

We remark that (3.15) contains all of the logarithmic terms in powers of ν in the outer expansion of the solution. However, it does not contain transcendentally small terms of algebraic, or mixed algebraic-logarithmic, order in ε as $\varepsilon \to 0$.

Next, in order to validate our infinite order logarithmic series result, we will determine the exact solution of (3.1)–(3.3) and then expand it for $\varepsilon \to 0$. Since the solutions to (3.1) proportional to $\sin\theta$ are linear combinations of $\{\rho^3, \rho\log\rho, \rho, \rho^{-1}\}\sin\theta$, the solution to (3.1), which satisfies (3.2), is given in terms of two constants A and B by

$$u = \left(A\rho^3 + B\rho\log\rho + \left(-2A + \frac{1}{2} - \frac{B}{2}\right)\rho + \left(\frac{1}{2} + A + \frac{B}{2}\right)\frac{1}{\rho}\right)\sin\theta\,. \tag{3.16}$$

Upon imposing that $u = u_\rho = 0$ on $\rho = \varepsilon$, we obtain that A and B satisfy

$$A\varepsilon^3 + B\varepsilon\log\varepsilon + \left(-2A + \frac{1}{2} - \frac{B}{2}\right)\varepsilon + \kappa\varepsilon \;= 0\,, \tag{3.17}$$

$$3A\varepsilon^3 + B\varepsilon + B\varepsilon\log\varepsilon + \left(-2A + \frac{1}{2} - \frac{B}{2}\right)\varepsilon - \kappa\varepsilon \;= 0\,, \tag{3.18}$$

where $\kappa = \mathcal{O}(1)$ is defined by

$$\kappa\varepsilon^2 = \frac{1}{2} + A + \frac{B}{2}\,. \tag{3.19}$$

We add (3.17) and (3.18) to eliminate κ, and neglect the higher order $A\varepsilon^3$ terms. In addition, since $A \sim -(1+B)/2$ from (3.19), we obtain the approximate system

$$B + 2B\log\varepsilon \sim 4A - 1 + B\,, \qquad A \sim -(1+B)/2\,, \tag{3.20}$$

for A and B, which has the solution

$$B \sim \frac{3\nu}{2-\nu}\,, \qquad A = 1 - \frac{3}{2-\nu}\,, \qquad \text{where} \qquad \nu \equiv \frac{-1}{\log\left[\varepsilon e^{1/2}\right]}\,. \tag{3.21}$$

From (3.21) and (3.16), we obtain that the outer solution, valid for $\rho \gg \mathcal{O}(\varepsilon)$, is indeed precisely (3.15).

Finally, we show how to readily derive (3.15) by formulating an appropriate singularity structure for the outer problem in terms of a free parameter S, representing the strength of the singularity. Then, S is determined from matching the outer solution to an appropriate inner solution. To this end, we look for an outer solution $u_H = u_H(\rho,\theta;S)$ that satisfies

$$\Delta_\rho^2 u_H \;=\; 0\,, \quad 0 < \rho < 1\,, \tag{3.22}$$

$$u_H \;=\; \sin\theta\,, \quad \partial_\rho u_H = 0\,, \quad \text{on} \quad \rho = 1\,, \tag{3.23}$$

$$u_H \;\sim\; S\rho\log\rho\sin\theta\,, \quad \text{as} \quad \rho \to 0\,. \tag{3.24}$$

This problem has a unique solution since the singularity condition (3.24) eliminates the more singular term of order $\mathcal{O}(\rho^{-1})$ as $\rho \to 0$. Therefore, (3.24) provides the two required additional boundary conditions, together with those in (3.23), for the fourth order problem (3.22)–(3.24).

In terms of the unique solution for u_H, we define the regular part R of the singularity structure by

$$u_H \sim (S\rho\log\rho + R\rho + o(1))\sin\theta\,, \quad \text{as} \quad \rho \to 0\,. \tag{3.25}$$

The exact solution to (3.22)–(3.24) is readily calculated as

$$u_H = \left(S\rho\log\rho + R\rho + \alpha\rho^3\right)\sin\theta\,, \tag{3.26}$$

where R and α are determined explicitly in terms of S as

$$R = \frac{S}{2} + \frac{3}{2}\,, \qquad \alpha = -\frac{S}{2} - \frac{1}{2}\,. \tag{3.27}$$

In terms of the inner variable $r = \rho/\varepsilon$, the near-field behaviour of (3.26) for $\rho \to 0$ is

$$u_H \sim \varepsilon \left[Sr \log r + r\,(S \log \varepsilon + R) + \mathcal{O}(\varepsilon^2) \right] \sin\theta\,. \tag{3.28}$$

The requirement that the far-field behaviour of the inner solution match with (3.28) is the condition that determines S.

The condition (3.28) yields that the inner solution v is $v(r,\theta) = \varepsilon^{-1} u(\varepsilon r, \theta)$, and must satisfy

$$\Delta_r^2 v \;=\; 0\,, \quad r > 1\,, \tag{3.29}$$

$$v = v_r \;=\; 0\,, \quad \text{on} \quad r = 1\,, \tag{3.30}$$

$$v \;\sim\; Sr \log r \sin\theta\,, \quad \text{as} \quad r \to \infty\,. \tag{3.31}$$

The solution to (3.31) is unique since we have eliminated the possibility of $\mathcal{O}(r^3)$ growth at infinity. Therefore, (3.31) contains effectively two "boundary" conditions. The solution is

$$v = S\left[r \log r - \frac{r}{2} + \frac{1}{2r} \right] \sin\theta\,. \tag{3.32}$$

Upon requiring that the $\mathcal{O}(r)$ terms in (3.28) and εv agree, we obtain that S satisfies $S \log \varepsilon + R = -S/2$. Since $R = S/2 + 3/2$ from (3.27), we can readily solve for S. In this way, we obtain that the outer solution u_H from (3.26) is

$$u_H \sim \left(S\rho \log \rho + \frac{S}{\nu}\rho - \frac{1}{2}(1+S)\rho^3 \right) \sin\theta\,, \tag{3.33}$$

where

$$S = \frac{3\nu}{2-\nu}\,, \qquad R = \frac{S}{2} + \frac{3}{2} = \frac{S}{\nu}\,, \qquad \nu \equiv \frac{-1}{\log\left[\varepsilon e^{1/2}\right]}\,. \tag{3.34}$$

This expression, referred to as the hybrid result, agrees with that obtained in (3.15) from a direct infinite order logarithmic expansion of the solution.

The careful examination of this very simple model problem has shown that by formulating an outer problem with a parameter-dependent singularity structure, we are ultimately able to determine an approximate solution that contains all the logarithmic terms in powers of ν, while avoiding calculating each individual term in an expansion of S in powers of ν as in

$$S \sim \frac{3\nu}{2\,(1-\nu/2)} = \frac{3\nu}{2} \sum_{j=0}^{\infty} \left(\frac{\nu}{2} \right)^j\,, \qquad \text{for} \quad \varepsilon < e^{-1} \approx 0.3679\,. \tag{3.35}$$

To highlight the performance of (3.33) at finite ε, we define $f''(1)$ by $u_{\rho\rho} = f''(1)\sin\theta$ at $\rho = 1$ and in Fig. 2 we compare the exact, hybrid, and two-term result, for $f''(1)$ as a function of ε. The hybrid and two-term result for $f''(1)$, as obtained from (3.33)–(3.34) and (3.35), is

$$f''_H(1) = -2S - 3\,, \qquad f''_{2T}(1) = -3 - 3\nu\,. \tag{3.36}$$

The corresponding exact result is $f''_E(1) = 4A - 1$, where A satisfies (3.17)–(3.18).

We remark that for related nonlinear singularly perturbed biharmonic problems $\Delta_\rho^2 u = F(u)$ in an annulus, where exact solutions are unavailable, it is typically intractable to perform an infinite order logarithmic expansion of the solution and then analytically calculate the coefficients in this expansion one-by-one. Instead, by formulating an appropriate parameter-dependent singularity structure as in (3.24), numerical methods can be used to compute the regular part $R(S)$ of the singularity behavior in (3.25). In terms of $R(S)$, a transcendental equation can be derived for $S = S(\nu)$ that has the effect of summing the infinite logarithmic expansion of the solution. This hybrid asymptotic-numerical methodology is the approach we use to analyze the low Reynolds number flow problems in §4–§6.

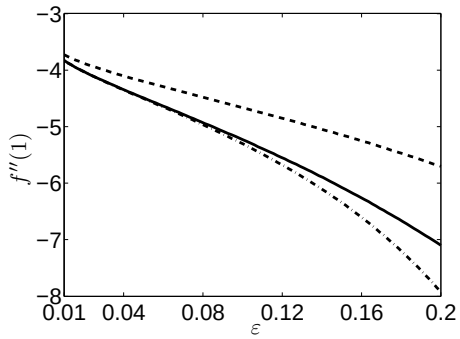

Figure 2. Plot of $f''(1)$ where $u = f(\rho)\sin\theta$ is either the exact or approximate solution to (3.1)–(3.3). The solid $(-)$ curve is the exact result from (3.16) and (3.17)–(3.18), while the $(-.)$ and $(--)$ curves are the hybrid and 2-term results, respectively, as obtained from (3.36).

4. Flow Past a Nanocylinder of Circular Cross-Section with a Rough Surface

Next, we study steady and incompressible flow of a Newtonian fluid around a nanocylinder of circular cross-section of radius L. In the far field the flow is uniform with speed U_∞ in the x-direction. We assume that the nanocylinder has roughness on its boundary. Therefore, slip occurs at the boundary and we replace the no-slip boundary condition by the Navier boundary condition. [Navier (1823)] proposed a slip boundary condition and claimed that the component of the fluid velocity tangent to the surface, v_θ, should be proportional to the rate of strain at the surface, $D_{r\theta} = 0.5(\partial v_\theta/\partial r - v_\theta/r + \partial v_r/(r\partial\theta))$. The degree of proportionality is determined by a constant l_c called the sliplength. With this modification of (2.1)–(2.3), the streamfunction ψ now satisfies (cf. [Matthews & Hill (2006)])

$$\Delta_r^2\psi \;=\; -\varepsilon\, J_r\left[\psi, \Delta_r\psi\right], \quad \text{for} \quad r > 1\,, \tag{4.1}$$

$$\psi \;=\; 0\,, \qquad l\psi_{rr} - \left(\frac{l}{r} + 1\right)\psi_r = 0\,, \quad \text{on} \quad r = 1\,, \tag{4.2}$$

$$\psi \;\sim\; r\sin\theta\,, \quad \text{as} \quad r \to \infty\,. \tag{4.3}$$

Here $\varepsilon \equiv U_\infty L\rho_f/\mu \ll 1$ is the Reynolds number and $l = l_c/L$ is the dimensionless sliplength.

We now use the hybrid approach of §2 to determine an asymptotic approximation to the solution of (4.1)–(4.3) that is accurate to all powers in $-1/\log\varepsilon$. In the outer region, we again set $\psi \sim \varepsilon^{-1}\Psi_H$, where Ψ_H satisfies (2.19)–(2.22) and has the local behaviour (2.26) as $\rho \to 0$. In terms of the Stokes variable $r = \rho/\varepsilon$, the local behaviour (2.26) yields

$$\psi \sim [Sr\log r + Sr\log\varepsilon + Rr]\sin\theta + \mathcal{O}(\varepsilon\log^2\varepsilon)\,. \tag{4.4}$$

The asymptotic matching condition is that the far-field behaviour as $r \to \infty$ of the Stokes solution must agree with (4.4).

In the Stokes region, where $r = \mathcal{O}(1)$, we set $\psi = S\psi_c$, where in place of (2.5)–(2.6), ψ_c now satisfies

$$\Delta_r^2\psi_c \;=\; 0\,, \quad \text{for} \quad r > 1\,, \tag{4.5}$$

$$\psi_c \;=\; 0\,, \qquad l\psi_{crr} - \left(\frac{l}{r} + 1\right)\psi_{cr} = 0\,, \quad \text{on} \quad r = 1\,, \tag{4.6}$$

$$\psi_c \;\sim\; r\log r\sin\theta\,, \quad \text{as} \quad r \to \infty\,. \tag{4.7}$$

The unique solution to (4.5)–(4.7) is

$$\psi_c = \left(r\log r + cr - \frac{c}{r}\right)\sin\theta\,, \quad \text{where} \quad c \equiv -\frac{1}{2+4l}\,. \tag{4.8}$$

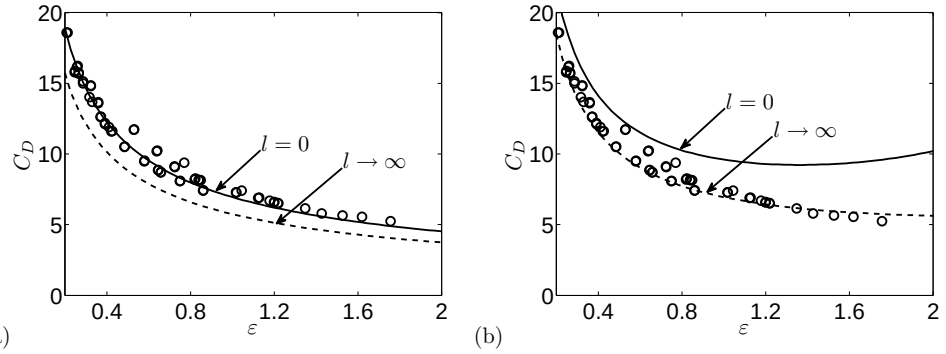

Figure 3. The drag coefficient C_D versus the Reynolds number ε for a circular nanocylinder; solid curve: $l = 0$; dashed curve: $l \to \infty$; $\circ$: experimental results of [Tritton (1959)] for $l = 0$. (a) The results of hybrid model. (b) The asymptotic result of [Matthews & Hill (2006)] (see (4.2) and (4.4) of [Matthews & Hill (2006)]).

Upon matching the $\mathcal{O}(r\sin\theta)$ terms in (4.4) and in the far-field behaviour of $\psi = S\psi_c$ from (4.8), we obtain that S satisfies

$$\frac{S}{R(S)} = \nu \equiv -\frac{1}{\log\left[\varepsilon e^{-c}\right]}, \qquad c = -\frac{1}{4l+2}. \tag{4.9}$$

In terms of $S = S(\nu)$, the drag coefficient accurate to all powers of ν is

$$C_D \sim 4\pi\varepsilon^{-1}S(\nu) = 4\pi\varepsilon^{-1}\nu R\left[S(\nu)\right]. \tag{4.10}$$

In Fig. 3 we show the hybrid result for the drag coefficient C_D versus the Reynolds number ε, as obtained from (4.9) and (4.10). As anticipated, the drag coefficient decreases with the presence of slip due to a reduced resistance at the boundary of the body. For $\varepsilon \to 0$, [Matthews & Hill (2006)] derived analytically the first three terms in the logarithmic expansion of the drag coefficient for flow over a nanocylinder with circular cross-section. With this three term approximation, they concluded that, unlike the results of no-slip, the results with complete slip (i.e. $l = \infty$) are in agreement with the low Reynolds number experimental data of [Tritton (1959)]. However, it should be emphasized that the experimental and theoretical drag coefficient for the case of no-slip are in good agreement only when we include all the logarithmic correction terms in the asymptotic approximation. The hybrid formulation is able to account for all such terms. Therefore, the discrepancy in the work of [Matthews & Hill (2006)] may arise not from the slip condition at the boundary, but instead from not including all the logarithmic corrections to the drag coefficient. As evidence for this claim, we remark that for $l = 0$ it was shown in Fig. 6 of [Kropinski *et al.* (1995)] that, on the range $0 < \varepsilon < 2$, the hybrid drag coefficient in Fig. 3(a) compares extremely favorably with the corresponding full numerical result for the drag coefficient as computed from the full problem (4.1)–(4.3). This suggests that in the original experiments of [Tritton (1959)] it is probably safe to assume that there was negligible slip on the boundary of the cylinder.

4.1. A Transcendentally Small Term

In [Keller & Ward (1996)] it was shown how to calculate a transcendentally small term in the asymptotic expansion of the streamfunction in the Stokes region for the case of no-slip on the boundary of a cylinder of circular cross-section. Here, we consider the analogous problem for the case of slip, and we then extrapolate our result to finite ε to predict the value of the Reynolds number for which an eddy forms near the body.

In the Stokes region, we construct a higher order expansion of the solution in the form

$$\psi = S\psi_c + \varepsilon\psi_1 + \cdots, \tag{4.11}$$

where ψ_c is given by (4.8). Upon substituting (4.11) into (4.1) and (4.2), and using (4.8) to calculate the Jacobian, we obtain that

$$\Delta_r^2\psi_1 \;=\; -J_r\left[S\psi_c, S\Delta_r\psi_c\right] = -S^2\left[2\log r + (1+2c)\right]\frac{\sin(2\theta)}{r^2}\,, \quad \text{for } \; r>1\,, \tag{4.12}$$

$$\psi_1 \;=\; 0\,, \qquad l\psi_{1rr} - \left(\frac{l}{r}+1\right)\psi_1 = 0\,, \quad \text{on} \quad r=1\,. \tag{4.13}$$

Imposing that $\psi_1 = \mathcal{O}\left[(r\log r)^2\right]$ as $r\to\infty$, the solution to (4.12) has the form

$$\psi_1 = S^2\left[\frac{1}{16}\left(r\log r\right)^2 + \left(\frac{1}{32}+\frac{c}{8}\right)r^2\log r\right]\sin(2\theta) + \left(d_1 r^2 + d_2 + \frac{d_3}{r^2}\right)\sin(2\theta)\,, \tag{4.14}$$

for arbitrary constants d_1, d_2, and d_3.

Upon satisfying the boundary conditions in (4.13), we obtain after a lengthy, but straightforward, calculation that the solution to (4.12)–(4.13) in terms of one free parameter d_1 is

$$\begin{aligned}\psi_1 \;=\; \frac{S^2}{32}&\left[2\left(r\log r\right)^2 + \left(\frac{2l-1}{2l+1}\right)r^2\log r + \frac{\gamma_0}{2}\left(1-\frac{1}{r^2}\right)\right]\sin(2\theta)\\ &+d_1\left(r^2 - \left(\frac{2+4l}{1+4l}\right) + \frac{1}{r^2(1+4l)}\right)\sin(2\theta)\,,\end{aligned} \tag{4.15}$$

where γ_0 is defined in terms of l by

$$\gamma_0 = \frac{12l^2+1}{(1+2l)(1+4l)}\,. \tag{4.16}$$

The two-term Stokes expansion is $\psi = S\psi_c + \varepsilon\psi_1 + \cdots$. From (4.8) and (4.15)–(4.16), we obtain that the far-field behaviour for $r\gg 1$ of the Stokes expansion is

$$\begin{aligned}\psi \;\sim\; &\left[Sr\log r + Scr + o(1)\right]\sin\theta\\ &+\varepsilon\left[\frac{S^2}{32}\left(2(r\log r)^2 + \left(\frac{2l-1}{2l+1}\right)r^2\log r\right) + d_1 r^2 + \mathcal{O}(1)\right]\sin(2\theta) + \cdots\,.\end{aligned} \tag{4.17}$$

In contrast, the near-field behaviour as $\rho\to 0$ of the outer hybrid solution $\psi\sim\varepsilon^{-1}\Psi_H$ is determined from (2.26). Upon writing this result in terms of $r=\varepsilon^{-1}\rho$ we conclude that (4.17) must asymptotically match with

$$\begin{aligned}\psi \;\sim\; &\left[Sr\log r + r\left(S\log\varepsilon + R\right)\right]\sin\theta + \frac{\varepsilon S^2 r^2}{16}\left(\log^2 r + 2\log r\log\varepsilon + \log^2\varepsilon\right)\\ &+\frac{\varepsilon}{8}\left(SR + \frac{S^2}{4}\right)\left(r^2\log\varepsilon + r^2\log r\right)\sin(2\theta) + \varepsilon r^2\mathcal{C}_2\sin(2\theta)\,.\end{aligned} \tag{4.18}$$

The $r\sin\theta$ terms in (4.17) and (4.18) match when $Sc = S\log\varepsilon + R$, which yields (4.9). It is readily seen that the $\mathcal{O}((r\log r)^2)$ terms in (4.17) and (4.18) match identically. In addition, the $\mathcal{O}(r^2\log r)$ terms also match identically, since with $R = Sc - S\log\varepsilon$, the matching condition for these terms, given by,

$$\frac{S^2}{8}\log\varepsilon + \frac{1}{8}\left(SR + \frac{S^2}{4}\right) = \frac{S^2}{32}\left(\frac{2l-1}{2l+1}\right)\,, \tag{4.19}$$

reduces to $1+4c = (2l-1)/(2l+1)$. This yields $c=-1/(2+4l)$ in agreement with (4.8).

Finally, upon matching the $\mathcal{O}(r^2)$ terms in (4.17) and (4.18), we determine d_1 in terms of $\mathcal{C}_2$ as

$$d_1 = \frac{S^2}{16}\left(\log\varepsilon\right)^2 + \frac{1}{8}\left(SR + \frac{S^2}{4}\right)\log\varepsilon + \mathcal{C}_2\,. \tag{4.20}$$

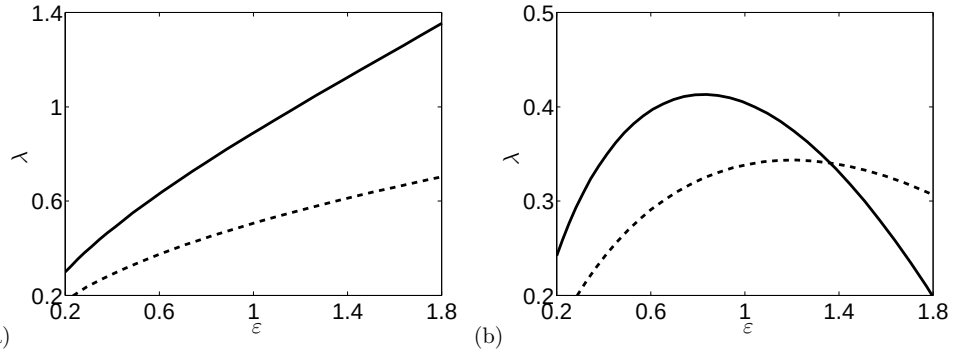

Figure 4. Plot of the asymmetry parameter λ versus ε for $l = 0$ (solid curve) and $l \to \infty$ (dashed curve). (a) Computed from the hybrid formulation (4.25) and (4.26). (b) The two-term approximation (4.29) for $l = 0$ (solid curve) and $l \to \infty$ (dashed curve).

With $R = Sc - S\log\varepsilon$ and $\log\varepsilon = c - 1/\nu$, (4.20) can be reduced to

$$d_1 = \frac{S^2}{16}\left(c - \frac{1}{\nu}\right)\left(c + \frac{1}{2} + \frac{1}{\nu}\right) + \mathcal{C}_2\,, \qquad c = \frac{-1}{2+4l} \qquad \nu = -\frac{1}{\log\left(\varepsilon e^{-c}\right)}\,. \tag{4.21}$$

Recall that $\mathcal{C}_2 = \mathcal{C}_2(S)$, as computed numerically from the hybrid outer problem (2.19)–(2.22), is plotted in Fig. 1(b). With d_1 specified in terms of $\mathcal{C}_2 = \mathcal{C}_2(S)$ from (4.21), the determination of the inner solution ψ_1 in (4.15)–(4.16) is complete. We then write the two-term inner expansion as

$$\psi \sim \hat{\psi}_0 \sin\theta + \varepsilon\hat{\psi}_1 \sin(2\theta) \sim \left(\hat{\psi}_0 + 2\varepsilon\hat{\psi}_1\cos\theta\right)\sin\theta\,, \tag{4.22}$$

where $\hat{\psi}_0 = \hat{\psi}_0(r)$ and $\hat{\psi}_1 = \hat{\psi}_1(r)$ can be identified from (4.8) and (4.15)–(4.16).

Equation (4.22) determines the weak upstream/downstream asymmetry in the flow field near the nanocylinder of circular cross-section. The streamline $\psi = 0$ consists of the circle $r = 1$, the rays $\theta = 0$ and $\theta = \pi$, and the boundary of an eddy if there is one. From (4.22), the equation of this boundary is

$$\sec\theta = -2\varepsilon\frac{\hat{\psi}_1}{\hat{\psi}_0}\,. \tag{4.23}$$

As ε increases, the eddy will first appear at the smallest ε for which the right-hand side of (4.23) attains the value 1 at $r = 1$. As such, we define the asymmetry parameter $\lambda(\varepsilon)$ by

$$\lambda(\varepsilon) = -2\varepsilon\lim_{r\to 1}\frac{\hat{\psi}_1}{\hat{\psi}_0}\,. \tag{4.24}$$

Extrapolating our $\varepsilon \ll 1$ theory to finite ε, we predict that an eddy forms when $\lambda(\varepsilon)$ crosses above 1. Upon using L'Hopital's rule we get $\lambda(\varepsilon) = -2\varepsilon\hat{\psi}_1'(1)/\hat{\psi}_0'(1)$ when $l > 0$. Finally, upon using (4.8) and (4.15)–(4.16) to calculate this ratio, we obtain after a lengthy, but straightforward, calculation that

$$\lambda(\varepsilon) = -\frac{\varepsilon}{1+4l}\left[\frac{S}{16}(10l-1) + \frac{8d_1}{S}(1+2l)\right]\,, \tag{4.25}$$

where d_1 is given in terms of $\mathcal{C}_2$ by (4.21).

In the special case of a no-slip boundary where $l = 0$, then $c = -1/2$ and (4.25) reduces to the result

$$\lambda(\varepsilon) = \frac{\varepsilon S}{2\nu^2}\left(1 + \frac{\nu}{2} + \frac{\nu^2}{8} - \frac{16\nu^2\mathcal{C}_2}{S^2}\right)\,, \tag{4.26}$$

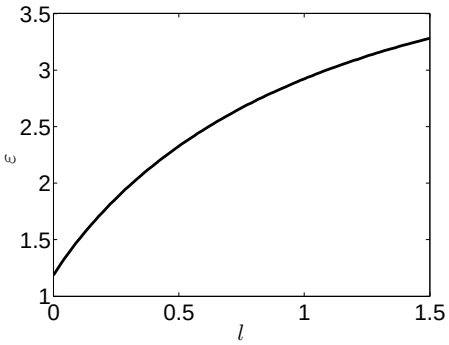

Figure 5. The critical value ε_c of the Reynolds number ε versus the sliplength l for which an eddy first forms near the cylinder. This curve was obtained by enforcing $\lambda[\varepsilon_c] = 1$, where $\lambda(\varepsilon)$ is the asymmetry parameter defined in (4.25).

which was derived in [Keller & Ward (1996)].

Next, we determine a two-term expansion in ν for $\lambda(\varepsilon)$ for any $l \geq 0$. We first obtain from (4.21) that

$$d_1 \sim \frac{S^2}{16}\left(-\frac{1}{\nu^2} - \frac{1}{2\nu} + \mathcal{O}(1)\right) + \mathcal{C}_2\,, \tag{4.27}$$

where the $\mathcal{O}(1)$ term depends on c, and hence the slip length. From (4.25), we obtain that

$$\lambda(\varepsilon) \sim \frac{\varepsilon S(1+2l)}{2\nu^2(1+4l)}\left[1 + \frac{\nu}{2} + \mathcal{O}(\nu^2) - \frac{16\mathcal{C}_2\nu^2}{S^2}\right]. \tag{4.28}$$

Then, we use $\mathcal{C}_2 \sim S(a_2 + 1/2)/8$ from (2.27), and $S \sim \nu(1 + a_2\nu)$ as obtained from (2.29) and (4.9). In this way, (4.28) reduces to

$$\lambda(\varepsilon) \sim \frac{\varepsilon(1+2l)}{2\nu(1+4l)}\left[1 - \nu\left(a_2 + \frac{1}{2}\right) + \mathcal{O}(\nu^2)\right], \tag{4.29}$$

where a_2 is defined in (2.16).

Finally, for the case of no slip $l = 0$, it can readily be shown that (4.29) is asymptotically equivalent to the result

$$\lambda \sim \frac{\varepsilon}{2\delta}\left[1 - \frac{\delta}{2} + \mathcal{O}(\delta^2)\right], \qquad \delta \equiv -\frac{1}{\left[a_2 + \log\left(\varepsilon e^{1/2}\right)\right]}, \tag{4.30}$$

as derived in [Skinner (1975)].

In summary, to calculate $\lambda(\varepsilon)$ we first determine $S = S(\nu)$ from the transcendental relation (4.9). Then, with $\mathcal{C}_2(S)$ computed numerically from the local behaviour of Ψ_H in (2.26), we calculate $\mathcal{C}_2(S(\nu))$, which yields d_1 from (4.21). This determines $\lambda(\varepsilon)$ from (4.25) when $l > 0$, and from (4.26) when $l = 0$. In Fig. 4(a) we plot $\lambda(\varepsilon)$ in (4.25) and (4.26) versus ε for the case $l = 0$ of a no-slip boundary and for the case $l = \infty$ corresponding to complete slip. In Fig. 4(b) we plot the corresponding two-term approximations for $\lambda(\varepsilon)$, as given in (4.29), for $l = 0$ and $l = \infty$. We conclude that the two-term approximations for $\lambda(\varepsilon)$ are rather inaccurate at finite ε, and since $\lambda < 1$ they do not predict the formation of an eddy. However, from the results in Fig. 4(a) that are accurate to all logarithmic terms, we conclude that $\lambda = 1$ when $\varepsilon = \varepsilon_c \approx 1.2$ and $l = 0$. This corresponds to the smallest Reynolds number ε for which an eddy first forms with no boundary slip. In Table 1 of [Sen *et al.* (2009)] the existing literature regarding the onset of separation (i.e., the generation of standing eddy) for low Re number flow past a circular cylinder is summarized. Separation occurs at about $Re = 2.5$ when the Re number is based upon the radius of the cylinder. From comparing the two curves in Fig. 4(a), we predict that the critical value of the Reynolds number ε for which an eddy first forms increases as the sliplength l increases. An eddy forms when the fluid lacks sufficient

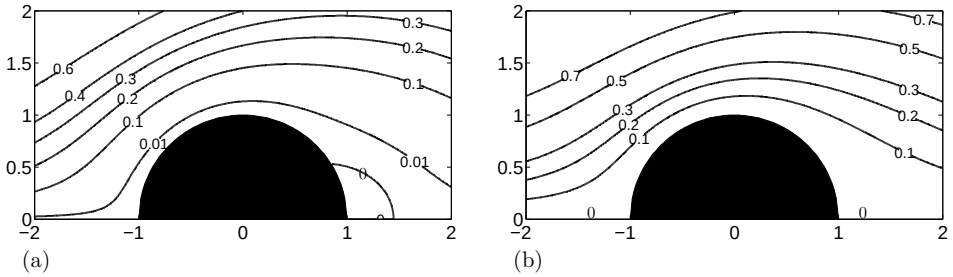

Figure 6. Contour plots of the stream function computed from (4.22) with $\varepsilon = 1.5$. The plot shows the flow asymmetry. (a) $l = 0$ (no slip). (b) $l = \infty$ (complete slip).

momentum to overcome the adverse pressure gradient at the rear of the cylinder. In the presence of slip, the drag force is smaller and consequently the momentum reduction is smaller in the region of adverse pressure gradient. This delays the separation of the boundary layer or the formation of any eddy. In Fig. 5 we plot the critical value ε_c of ε versus l at which an eddy first forms, as obtained from solving $\lambda[\varepsilon_c] = 1$ by Newton's method. Indeed this critical value increases as l increases.

In Fig. 6(a) and Fig. 6(b) we show a contour plot of the two-term expansion (4.22) at the finite value $\varepsilon = 1.5$ for $l = 0$ and $l = \infty$, respectively. This two-term expansion contains the transcendentally small effect of upstream/downstream asymmetry in the flow field in the Stokes region for $\varepsilon \ll 1$. At $\varepsilon = 1.5$, Fig. 6(a) shows the existence of an eddy for the no-slip case. At this value of ε, Fig. 6(b) shows that there is no eddy for the complete slip case $l = \infty$. Finally, we remark that although the correction term ψ_1 determines upstream/downstream asymmetry of the flow field, it does not contribute to further transcendentally small correction terms to the drag coefficient (cf. [Skinner (1975)], [Keller & Ward (1996)]).

5. Flow Past a Porous Circular Cylinder

Next, we study steady and incompressible low Reynolds number flow of a Newtonian fluid around a porous cylinder of circular cross-section with cross-sectional radius L. At large distances from the body the speed of the flow is U_∞ in the x direction. We solve the Navier Stokes equation outside the cylinder and the Brinkman equation inside the cylinder (i.e. in the porous region). The Brinkman equation is a governing equation for flow through a porous medium in which a viscous term is added to the classical Darcy equation. On the surface of the cylinder, we assume the continuity of velocity and stress.

We adopt a polar coordinate system located at the centre of the cylinder, similar to §4. In terms of dimensionless variables, the governing system in terms of the Stokes (inner) variable r is (cf. [Kohr *et al.* (2009)])

$$\Delta_r^2 \psi^e + \varepsilon J_r\left[\psi^e, \Delta_r \psi^e\right] = 0\,, \quad \text{for} \quad r > 1\,, \tag{5.1}$$

$$\Delta_r\left(\Delta_r - \chi^2\right)\psi^i = 0\,, \quad \text{for} \quad 0 \le r < 1\,, \tag{5.2}$$

$$\psi^e = \psi^i\,, \qquad \frac{\partial \psi^e}{\partial r} = \frac{\partial \psi^i}{\partial r}\,, \quad \text{on} \quad r = 1\,, \tag{5.3}$$

$$\frac{\partial^2 \psi^e}{\partial r^2} = \frac{\partial^2 \psi^i}{\partial r^2}\,, \quad \text{on} \quad r = 1\,, \tag{5.4}$$

$$\frac{\partial^3 \psi^e}{\partial r^3} - \frac{\partial^3 \psi^i}{\partial r^3} = -\chi^2 \frac{\partial \psi^i}{\partial r}\,, \quad \text{on} \quad r = 1\,, \tag{5.5}$$

$$\psi^e \sim r\sin\theta\,, \quad \text{as} \quad r \to \infty\,. \tag{5.6}$$

The derivation of this system is given in Appendix B.

Here we have chosen superscripts i and e, which denote internal flow (where $r < 1$) and external flow (where $r > 1$), respectively. Equation (5.2) is the non-dimensional Brinkman equation in terms of the stream function ψ defined inside the porous cylinder. The condition (5.3) specifies the continuity of the normal and tangential velocity components on the boundary of cylinder. The continuity of the tangential and normal stress are specified by (5.4) and (5.5). The two dimensionless parameters in this system are the Reynolds number $\varepsilon \equiv U_\infty L\rho_f/\mu$ and the Darcy number Da, with the latter defined by

$$Da = 1/\chi^2\,, \qquad \chi \equiv L/\sqrt{k}\,. \tag{5.7}$$

Here k is the permeability of the porous cylinder and L is the radius of the cylinder cross-section.

To determine the drag coefficient for this problem accurate to all orders in $-1/\log\varepsilon$ we proceed as in §4. In the outer region, we write $\psi = \varepsilon^{-1}\Psi_H$, where Ψ_H satisfies (2.19)–(2.22). Therefore, the matching condition for the far-field behaviour of the inner solution to (5.1)–(5.6) is that

$$\psi \sim [Sr\log r + Sr\log\varepsilon + Rr]\sin\theta\,, \tag{5.8}$$

where $R = R(S)$ is determined from the hybrid outer problem (2.19)–(2.22) (cf. Fig. 1(a)).

Therefore, in the inner region we write $\psi = S\psi_c + \mathcal{O}(\varepsilon)$, where $\psi_c \sim r\log r\sin\theta$ as $r \to \infty$. From (5.1)–(5.6), ψ_c satisfies

$$\Delta_r^2\psi_c^e = 0\,, \quad \text{for} \quad r > 1\,, \tag{5.9}$$

$$\Delta_r\left(\Delta_r - \chi^2\right)\psi_c^i = 0\,, \quad \text{for} \quad 0 \le r < 1\,, \tag{5.10}$$

$$\psi_c^e = \psi_c^i\,, \qquad \frac{\partial\psi_c^e}{\partial r} = \frac{\partial\psi_c^i}{\partial r}\,, \quad \text{on} \quad r = 1\,, \tag{5.11}$$

$$\frac{\partial^2\psi_c^e}{\partial r^2} = \frac{\partial^2\psi_c^i}{\partial r^2}\,, \quad \text{on} \quad r = 1\,, \tag{5.12}$$

$$\frac{\partial^3\psi_c^e}{\partial r^3} - \frac{\partial^3\psi_c^i}{\partial r^3} = -\chi^2\frac{\partial\psi_c^i}{\partial r}\,, \quad \text{on} \quad r = 1\,, \tag{5.13}$$

with $\psi_c^e \sim r\log r\sin\theta$ as $r \to \infty$.

The solution to this problem has the form

$$\psi_c = \begin{cases} (r\log r + cr + b/r)\sin\theta\,, & r > 1\,, \\ (e_1 r + e_2 I_1(\chi r))\sin\theta\,, & 0 \le r < 1\,, \end{cases} \tag{5.14}$$

where $I_1(z)$ is the modified Bessel function of the first kind of order one. The conditions (5.11)-(5.13) yield the four equations for c, b, e_1, and e_2, given by

$$c + b = e_1 + e_2 I_1(\chi)\,, \qquad 1 + c - b = e_1 + e_2\chi I_1'(\chi)\,, \tag{5.15}$$

$$1 + 2b = e_2\chi^2 I_1''(\chi)\,, \qquad -1 - 6b - e_2\chi^3 I_1'''(\chi) = -\chi^2\left(e_1 + e_2\chi I_1'(\chi)\right)\,. \tag{5.16}$$

We solve (5.15) for c and b in terms of e_1 and e_2. Upon using the identities that $\chi I_1'(\chi) = \chi I_0(\chi) - I_1(\chi)$ and $I_2(\chi) = I_0(\chi) - 2I_1(\chi)/\chi$, we obtain that

$$c = \frac{1}{2}\left[2e_1 - 1 + e_2\chi I_0(\chi)\right]\,, \qquad b = \frac{1}{2}\left[1 + e_2\left(2I_1(\chi) - \chi I_0(\chi)\right)\right]\,. \tag{5.17}$$

Upon substituting b from (5.17) into the first of (5.16), we get $e_2\left[\chi^2 I_1'' + \chi I_0 - 2I_1\right] = 2$. Then, since $\chi^2 I_1'' = -\chi I_1' + (\chi^2+1)I_1$ and $\chi I_1' + I_1 = \chi I_0$, we conclude that

$$e_2 = 2/\left[\chi^2 I_1(\chi)\right]\,. \tag{5.18}$$

To determine e_1, we substitute (5.18) and b from (5.17) into the second equation of (5.16). This yields

$$\chi^2 e_1 = -2 + \frac{2}{I_1(\chi)}\left[\chi I_1''' + 3I_1'' - \chi I_1'\right]\,. \tag{5.19}$$

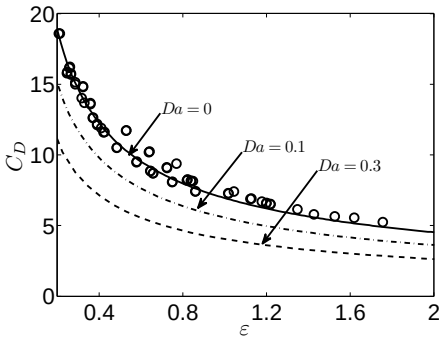

Figure 7. Drag coefficient C_D versus Reynolds number ε for a circular porous cylinder, as obtained from (5.22) and (5.23). The solid lines are the hybrid results for $Da = 0$, $Da = 0.1$ and $Da = 0.3$. $\circ$ shows the experimental result of [Tritton (1959)] for an impermeable cylinder of circular cross-section with no slip.

After using standard identities to express the derivatives of I_1 in terms of I_1 and I_0, we obtain that

$$e_1 = 2/\chi^2 \,. \tag{5.20}$$

Finally, we substitute (5.18) and (5.20) into (5.17) to determine c and b as

$$c = -\frac{1}{2} + \frac{2}{\chi^2} + \frac{I_0(\chi)}{\chi I_1(\chi)} \,, \qquad b = \frac{1}{2} + \frac{2}{\chi^2} - \frac{I_0(\chi)}{\chi I_1(\chi)} \,. \tag{5.21}$$

With c, b, e_1, and e_2 determined from (5.18), (5.20), and (5.21), the inner solution ψ_c is known from (5.14).

The matching condition between the far-field as $r \to \infty$ of ψ_c and (5.8) is that the $r\sin\theta$ terms in (5.8) and in the expression (5.14) for $r > 1$ must agree. This yields that $S = S(\nu)$ satisfies the transcendental relation

$$\frac{S}{R(S)} = \nu \equiv -\frac{1}{\log\left[\varepsilon e^{-c}\right]} \,, \qquad c = -\frac{1}{2} + \frac{2}{\chi^2} + \frac{I_0(\chi)}{\chi I_1(\chi)} \,. \tag{5.22}$$

In terms of $S = S(\nu)$, the drag coefficient accurate to all powers of ν is given by

$$C_D \sim 4\pi\varepsilon^{-1} S(\nu) = 4\pi\varepsilon^{-1}\nu R\left[S(\nu)\right] \,. \tag{5.23}$$

Therefore, the results (4.9) and (4.10) obtained in §4 for the nanocylinder with slip still apply provided that we simply re-define c in (4.9) by the expression in (5.22).

In the limit $\chi \to \infty$, for which $Da \to 0$, we use the large argument expansion of I_0 and I_1 in (5.22) to get $c = -1/2 + \mathcal{O}(\chi^{-1})$. Therefore, for a cylinder with very small permeability, the drag coefficient in (5.23) reduces, as expected, to the drag coefficient in (4.10) with no slip (i.e. $l = 0$). In the limit $\chi \to 0$, for which $Da \to +\infty$, then $c = 4/\chi^2 + \mathcal{O}(1)$. Since $c \gg 1$ in this limit, it follows from (5.23) that the drag coefficient for a very permeable cylinder is much lower than that for an impermeable cylinder.

In Fig. 7 we plot C_D versus ε, as obtained from (5.22) and (5.23), for different values of the Darcy number Da. We observe that the drag coefficient decreases as the Darcy number increases (i.e. as the permeability increases). The increase in the permeability results in less resistance to the fluid flow around the cylinder and, consequently, leads to a reduction in the drag force.

5.1. A Transcendentally Small Term

We now show how to calculate a transcendentally small term in the Stokes region. In the Stokes region, we expand the solution as

$$\psi = S\psi_c + \varepsilon\psi_1 + \cdots \,, \tag{5.24}$$

where ψ_c is given by (5.14). Upon substituting (5.24) and (5.14) into (5.1)–(5.6), and calculating the Jacobian, we obtain that

$$\Delta_r^2\psi_1^e = -J_r\left[S_c\psi_c^e, S_c\Delta_r\psi_c^e\right] \;=\; -S^2\left[2\log r + (1+2c)\right]\frac{\sin(2\theta)}{r^2}\,, \quad \text{for } r>1\,, \tag{5.25}$$

$$\Delta_r\left(\Delta_r - \chi^2\right)\psi_1^i \;=\; 0\,, \quad \text{for} \quad 0\le r<1\,, \tag{5.26}$$

subject to the continuity conditions (5.3)–(5.5), and the far-field behavior $\psi_1^e = \mathcal{O}\left[(r\log r)^2\right]\sin(2\theta)$ as $r\to\infty$. For $r>1$, we note that the problem (5.25) for ψ_1^e is the same as for the corresponding nanocylinder problem (4.12), except that c is now given as in (5.22).

The solution for ψ_1 is given in terms of the five constants d_1, d_2, d_3, f_1, and f_2, by

$$\psi_1 = \begin{cases} S^2\left[\frac{1}{16}\left(r\log r\right)^2 + \left(\frac{1}{32}+\frac{c}{8}\right)r^2\log r\right]\sin(2\theta) + \left(d_1r^2 + d_2 + \frac{d_3}{r^2}\right)\sin(2\theta)\,, \;\; r>1\,, \\ \left(f_1r^2 + f_2I_2(\chi r)\right)\sin(2\theta)\,, \quad 0<r<1\,, \end{cases} \tag{5.27}$$

where $I_2(z)$ is the modified Bessel function of the first kind of order two. As similar to the analysis in §4.1, the far-field behavior as $r\to\infty$ of $S\psi_c + \varepsilon\psi_1$ must match with (4.18). It readily follows that the $r^2\log^2 r\sin(2\theta)$ and $r^2\log r\sin(2\theta)$ terms in this matching condition agree automatically when S satisfies (5.22). In contrast, the $r^2\sin(2\theta)$ terms agree when

$$d_1 = \frac{S^2}{16}\left(c-\frac{1}{\nu}\right)\left(c+\frac{1}{2}+\frac{1}{\nu}\right) + \mathcal{C}_2\,, \qquad \nu = -\frac{1}{\log\left(\varepsilon e^{-c}\right)}\,, \tag{5.28}$$

where c is given in (5.22), and $\mathcal{C}_2(S)$ is to be computed from the hybrid problem (2.19)–(2.22) (cf. Fig. 1(b)).

To determine the remaining constants d_2, d_3, f_1, and f_2, in (5.27) in terms of the now known d_1, we simply impose the four continuity conditions in (5.3)–(5.5) for ψ_1. This yields the four equations

$$d_1 + d_2 + d_3 = f_1 + f_2I_2(\chi)\,, \tag{5.29}$$

$$2d_1 - 2d_3 + \frac{S^2}{32}\left(1+4c\right) = 2f_1 + f_2\chi I_2'(\chi)\,, \tag{5.30}$$

$$2d_1 + 6d_3 + \frac{3S^2}{32}\left(1+4c\right) = 2f_1 + f_2\chi^2 I_2''(\chi)\,, \tag{5.31}$$

$$S^2\left(\frac{5}{16}+\frac{c}{4}\right) - 24d_3 - f_2\chi^3 I_2'''(\chi) = -\chi^2\left(2f_1 + f_2\chi I_2'(\chi)\right)\,. \tag{5.32}$$

From (5.29) and (5.30) we can isolate d_2 and d_3 in terms of f_1 and f_2. In this way, and by using the identity $2I_2 + \chi I_2' = \chi I_1$, we obtain that

$$d_2 \;=\; -2d_1 - \frac{S^2}{64}\left(1+4c\right) + 2f_1 + \frac{f_2\chi I_1(\chi)}{2}\,, \tag{5.33}$$

$$d_3 \;=\; d_1 + \frac{S^2}{64}\left(1+4c\right) - f_1 - f_2\left(\frac{\chi I_1(\chi)}{2} - I_2(\chi)\right)\,, \tag{5.34}$$

where d_1 is given in (5.28).

Finally, upon substituting (5.33) and (5.34) into (5.31) and (5.32), we can determine f_1 and f_2 in terms of d_1 given in (5.28). After a lengthy, but straightforward, calculation, we conclude

$$f_1 \;=\; \beta\left[-I_0(\chi)\left(\frac{S^2}{32}+\frac{cS^2}{16}\right) - I_2(\chi)\left(d_1 + \frac{3S^2}{128} + \frac{3cS^2}{32}\right)\right]\,, \tag{5.35}$$

$$f_2 \;=\; \beta\left[d_1 + \frac{S^2}{4}\left(\frac{3}{32}+\frac{1}{\chi^2}\right) + \frac{cS^2}{2}\left(\frac{3}{16}+\frac{1}{\chi^2}\right)\right]\,, \tag{5.36}$$

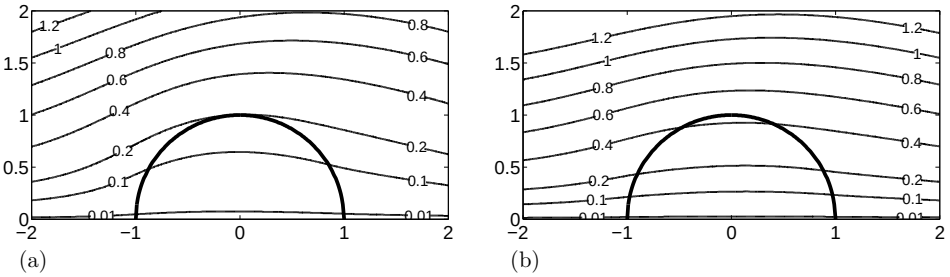

Figure 8. Contour plots of the stream function computed from the two term expansion obtained from (5.24), (5.14) and (5.27)) with $\varepsilon = 1.5$. The circular boundary of the porous cylinder is shown. The plot shows only a rather mild flow-field asymmetry in the Stokes region. (a) $Da = 0.1$ (b) $Da = 0.3$.

where β is defined by

$$\beta \equiv \left(I_2(\chi) + \frac{\chi^2 I_0(\chi)}{8} \right)^{-1} , \tag{5.37}$$

and c is defined in (5.21). Then, d_2 and d_3 can be calculated from (5.33) and (5.34). This completes the determination of ψ_1 in (5.27).

For $\varepsilon = 0.15$, in Fig. 8(a) and Fig. 8(b) we show a contour plot of the two-term expansion (5.24) for the streamfunction when $Da = 0.1$ and $Da = 0.3$, respectively. As Da increases, corresponding to an increase in the permeability of the cylinder, more fluid flows through the porous cylinder. The volume rate of flow in the porous cylinder can be obtained by subtracting the values of the streamfunction surrounding the cylinder. In contrast to the case of an impermeable cylinder with and without slip at the same Reynolds number of $\varepsilon = 1.5$ shown in Fig. 6, we observe only a relatively weak upstream/downstream asymmetry in the flow field for the porous cylinder when either $Da = 0.1$ or $Da = 0.3$.

6. Flow Past Two Identical Circular Cylinders

In this section we study steady incompressible low Reynolds number flow past two parallel identical cylinders. The cross-section of each cylinder is assumed to be a circle of radius L, centered on the x-axis, with a center-to-center separation distance of dL with $d \geq 2$. We assume a no-slip condition on the boundary of the two cylinders. In the far-field, the flow is assumed to be uniform in the x direction with speed U_∞. We non-dimensionalize lengths by L and the flow velocity by U_∞ to obtain the Reynolds number $\varepsilon = U_\infty L \rho_f / \mu$, where ρ_f is the density and μ the dynamic viscosity.

In terms of the Stokes variable $\mathbf{y}$, with $r = |\mathbf{y}|$, the streamfunction ψ satisfies

$$\Delta^2 \psi \;=\; -\varepsilon \, J\left[\psi, \Delta\psi\right] , \quad \text{for} \quad \mathbf{y} \notin D , \tag{6.1}$$

$$\partial_s \psi \;=\; \partial_n \psi = 0 , \quad \mathbf{y} \in \partial D , \tag{6.2}$$

$$\psi \;\sim\; r \sin\theta , \quad \text{as} \quad r \to \infty . \tag{6.3}$$

Here $J\left[a, b\right] \equiv a_{y_1} b_{y_2} - a_{y_2} b_{y_1}$, where $\mathbf{y} = (y_1, y_2)^t = r(\cos\theta, \sin\theta)$. In addition, D is the union of the cross-sections of the two cylinders

$$D = D_0 \cup D_1 , \qquad D_0 = \{\mathbf{y} \,|\, |\mathbf{y} - \frac{d}{2} e_1| \leq 1\} \qquad D_1 = \{\mathbf{y} \,|\, |\mathbf{y} + \frac{d}{2} e_1| \leq 1\} , \tag{6.4}$$

where $e_1 = (1, 0)^t$. In (6.2), $\partial_s \psi_c$ denotes the tangential derivative to ∂D. In this symmetric case, where the cylinders have a common cross-sectional radius, we can replace $\partial_s \psi_c = 0$ on ∂D with the condition $\psi_c = 0$ on ∂D.

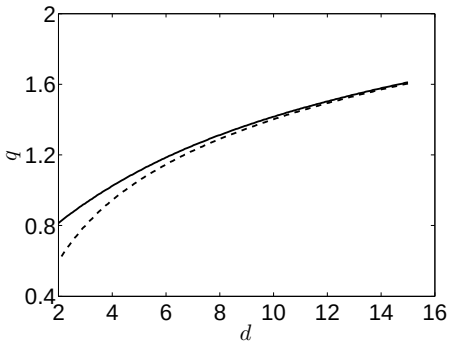

Figure 9. Plot of the parameter q versus the separation d between the centers of the circular cross-sections of the two cylinders. The solid line is the infinite series result (6.12), while the dashed line is its large d approximation (6.18).

With this parallel arrangement of the two cylinders with respect to the free stream, the flow field is symmetric in y_2. As such, our asymptotic analysis of (6.1)–(6.4) proceeds as in §2. In the outer Oseen region, the two cylinders are effectively replaced by a singularity at the origin. More specifically, we let $\psi = \varepsilon^{-1}\Psi_H$ and introduce the Oseen variable $\mathbf{x}$ defined by $\mathbf{x} = \varepsilon\mathbf{y}$. We obtain that Ψ_H satisfies the parameter-dependent hybrid problem (2.19)–(2.22). This leads to the following matching condition for the far-field behavior of the Stokes solution: ψ

$$\psi \sim [Sr\log r + (S\log\varepsilon + R)\, r]\sin\theta\,. \tag{6.5}$$

Here $r = |\mathbf{y}|$ is the Stokes variable and $R = R(S)$ is computed from the hybrid outer problem (2.19)–(2.22) (cf. Fig. 1(a)).

In order to match the Stokes solution to (6.5), we write $\psi = S\psi_c$, where ψ_c satisfies the Stokes problem

$$\Delta^2\psi_c = 0\,, \quad \mathbf{y}\notin D\,, \tag{6.6}$$

$$\psi_c = \partial_n\psi_c = 0\,, \quad \mathbf{y}\in\partial D\,, \tag{6.7}$$

$$\psi_c \sim r\log r\sin\theta\,, \quad \text{as} \quad r\to\infty\,. \tag{6.8}$$

In terms of the unique solution to this problem, we must calculate a constant q, depending on the distance d between the centers of the cross-sections of the cylinders, for which

$$\psi_c - r\log r\sin\theta \to -qr\sin\theta + o(1)\,, \qquad \text{as} \quad r\to\infty\,. \tag{6.9}$$

Then, by comparing (6.9) with the matching condition (6.5), and recalling that $\psi = S\psi_c$, we obtain in terms of q that $S = S(\nu)$ satisfies the transcendental equation

$$\frac{S}{R(S)} = \nu \equiv \frac{-1}{\log\left[\varepsilon e^{q}\right]}\,. \tag{6.10}$$

In terms of $S = S(\nu)$, the drag coefficient accurate to all powers of ν is

$$C_D \sim 4\pi\varepsilon^{-1}S(\nu)\,. \tag{6.11}$$

In [Umemura (1982)] an exact solution to (6.6)–(6.9) was obtained by first transforming the region using bipolar coordinates. From this solution the parameter q can be identified as

$$q = \frac{\log 2}{2} + \frac{1}{2}\log\left(\frac{d^2}{4} - 1\right) + \frac{1}{2}\sum_{m=1}^{\infty}(a_m + b_m)m\,, \tag{6.12}$$

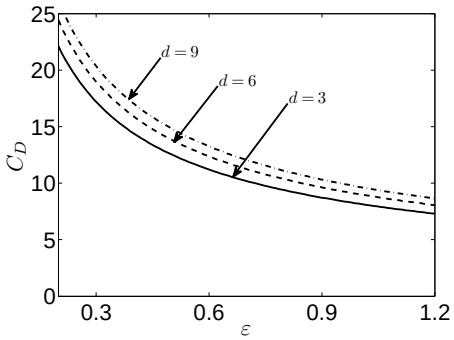

Figure 10. Drag coefficient C_D versus Reynolds number ε for two parallel identical circular cylinders for several values of the dimensionless distance $d > 2$ between the centers of the cylinders. The drag coefficient is computed from the hybrid formulation (6.10), (6.11) and (6.12)–(6.16).

where the coefficients a_m and b_m for $m \geq 1$ are defined by

$$a_m = \frac{1}{m+1}\left[\frac{-(m+1)+me^{-2\alpha}+e^{-2m\alpha}}{m\sinh(2\alpha)+\sinh(2m\alpha)}\right], \qquad m \geq 2\,, \tag{6.13}$$

$$b_m = \frac{1}{m-1}\left[\frac{-(m-1)+me^{2\alpha}-e^{-2m\alpha}}{m\sinh(2\alpha)+\sinh(2m\alpha)}\right], \qquad m \geq 2\,, \tag{6.14}$$

$$a_1 = \frac{-1}{1+e^{2\alpha}}\,, \qquad b_1 = \log 2 - \alpha - \frac{1}{2}e^{-2\alpha} + \frac{\cosh(2\alpha)}{1+e^{2\alpha}}\,. \tag{6.15}$$

Here α is related to d by

$$\alpha = \log\left(\frac{d}{2} + \sqrt{\frac{d^2}{4}-1}\right), \quad d \geq 2\,. \tag{6.16}$$

For $d \gg 1$, we readily derive from (6.12) that

$$q \sim \frac{1}{2}\log 2 + \frac{1}{2}\log\left(\frac{d^2}{4}\right) + \frac{b_1}{2}\,, \tag{6.17}$$

where $b_1 \sim -\log d + \log 2 + 1/2$. This yields that

$$q \sim \frac{1}{2}\log d + \frac{1}{4}\,, \quad \text{for} \quad d \gg 1\,. \tag{6.18}$$

In Fig. 9 we plot q versus d from (6.12) and compare it with the large d approximation (6.18). In Appendix C we outline the derivation of (6.12)–(6.16) from the formulation in [Umemura (1982)].

In Fig. 10 we plot the drag coefficient C_D, as obtained from (6.10), (6.11) and (6.12)–(6.16) for several values of the inter-separation distance $d > 2$.

7. Discussion

In this paper we have studied a few steady-state low Reynolds number flow problems in two dimensions with the goal of determining drag coefficients that are accurate to all orders in powers of $-1/\log\varepsilon$. In addition, we have shown how to calculate transcendentally small terms of order $\mathcal{O}(\varepsilon)$ in the Stokes region near the body, which predict the upstream/downstream asymmetry of the flow field near the body.

The analysis has revealed the central role of the solution Ψ_H of the hybrid problem (2.19)–(2.22) and its local behaviour (2.26), as given in Lemma 1, in terms of two functions $R(S)$ and $\mathcal{C}_2(S)$, which must be

computed numerically. Given that the hybrid problem is posed on $\rho > 0$, and has no length-scale, it is an interesting open problem to investigate whether the class of exact solutions to the two-dimensional Navier Stokes equations found using complex variable methods in [Ranger (1995)] can be used to determine these two functions $R(S)$ and $\mathcal{C}_2(S)$ analytically.

Secondly, if one can prove using rigorous PDE methods that $R(S)$ is analytic in some neighbourhood of $S = 0$ then, since $R(0) = 1 \neq 0$, the function $\mathcal{G}(S) \equiv S/R(S)$ must be analytic in some neighbourhood of $S = 0$, and hence have a convergent power series (Taylor series) expansion near $S = 0$. Then, by a reversion of series, it follows that $S = S(\nu)$, as obtained from the transcendental relation $\mathcal{G}(S) = \nu$ of either (2.24), (4.9), or (5.22), and consequently the associated drag coefficient, must have a convergent power series expansion for ν sufficiently small. This shows that, under an analyticity assumption on $R(S)$ for $|S| \ll 1$, a term-by-term expansion of the drag coefficient in powers of $-1/\log\varepsilon$ must generate a convergent, and not simply asymptotic, power series for $-1/\log\varepsilon$ sufficiently small.

Another open issue is to compare our asymptotic theory with full numerical simulations of the underlying PDE system to determine the accuracy of our prediction of critical values of the Reynolds number for the initial formation of an Eddy near the surface of the nanoparticle of §4. The critical values ε_c of the Reynolds number as a function of the sliplength were found to be $\mathcal{O}(1)$, and hence outside the range of validity of our small ε theory. However, we remark that for a no-slip boundary condition, it was shown in [Kropinski *et al.* (1995)] that the asymptotic drag coefficient as predicted by the hybrid theory compares very favorably with that from full numerical simulations up to $\varepsilon \approx 2$. It would be interesting to perform detailed full numerical computations to determine whether our asymptotic theory can quantitatively predict flow field asymmetry near the body at such $\mathcal{O}(1)$ values of ε.

Next, we discuss how our theoretical framework for treating infinite logarithmic expansions in low Reynolds number flow problems for flow past a cylinder of circular cross-section can be extended to flow past a cylinder of arbitrary cross-section. To treat such problems, where there is no symmetry with respect to the free stream, instead of (2.19)–(2.22) we must solve the following parameter-dependent outer hybrid problem where $\mathbf{S} = (S_1, S_2)^t$:

$$\Delta_\rho^2 \Psi_H = -J_\rho\left[\Psi_H, \Delta_\rho \Psi_H\right], \quad \rho > 0, \tag{7.1}$$

$$\Psi_H \sim \rho \sin\theta, \quad \text{as} \quad \rho \to \infty, \tag{7.2}$$

$$\Psi_H \sim \mathbf{S}\cdot\mathbf{x}\log\rho, \quad \text{as} \quad \rho = |\mathbf{x}| \to 0, \tag{7.3}$$

where $\rho = |\mathbf{x}|$ and $\mathbf{x} = \rho(\cos\theta, \sin\theta)^t$. In terms of this solution we must numerically compute $\mathbf{R}(\mathbf{S}) \equiv (R_1(S_1, S_2), R_2(S_1, S_2))^t$, defined from the limiting behavior

$$\Psi_H - \mathbf{S}\cdot\mathbf{x}\log\rho = \mathbf{R}(\mathbf{S})\cdot\mathbf{x}, \qquad \text{as} \quad \rho \to 0. \tag{7.4}$$

In terms of the inner Stokes variable $\mathbf{y} = \mathbf{x}/\varepsilon$, where $r = |\mathbf{y}|$, (7.4) yields the following matching condition for the far-field behavior of the Stokes solution:

$$\Psi_H \sim \varepsilon\left[\mathbf{S}\log|\mathbf{y}| + \mathbf{R} + \mathbf{S}\log\varepsilon\right]\cdot\mathbf{y}. \tag{7.5}$$

For concreteness, suppose that there is an impermeable cylinder of arbitrary cross-section with no slip on its boundary. Then, in the Stokes region, we write $\psi = \varepsilon\mathbf{S}\cdot\psi_c$, where ψ_c is the vector solution of

$$\Delta^2\psi_c = 0 \qquad \mathbf{y} \notin D_0, \tag{7.6}$$

$$\psi_c = \frac{\partial\psi_c}{\partial n} = 0, \qquad \mathbf{y} \in \partial D_0, \tag{7.7}$$

$$\psi_c \sim \mathbf{y}\log|\mathbf{y}|, \qquad \text{as} \quad |\mathbf{y}| \to \infty. \tag{7.8}$$

where D_0 is the cross-section of the cylinder written in terms of the Stokes variable. In terms of this solution, we must numerically compute a 2×2 matrix M, which depends on the shape of the body, and is defined by the far-field condition

$$\psi_c - \mathbf{y}\log|\mathbf{y}| \to -M\mathbf{y} + o(1), \qquad |\mathbf{y}| \to \infty. \tag{7.9}$$

In this way, the far-field behavior of the Stokes solution is

$$\psi \sim \varepsilon \left[\mathbf{S} \cdot \mathbf{y} \log |\mathbf{y}| - \mathbf{S} \cdot M\mathbf{y} \right] . \tag{7.10}$$

The matching condition is that (7.10) must agree with (7.5), which yields that $\mathbf{S} = (S_1, S_2)^t$ must satisfy the coupled nonlinear algebraic system

$$\mathbf{R}(\mathbf{S}) + \mathbf{S} \log \varepsilon = -M^t \mathbf{S} \,, \tag{7.11}$$

where t denotes transpose.

We emphasize that $\mathbf{R}(\mathbf{S}) = (R_1(S_1, S_2), R_2(S_1, S_2))$ is independent of the shape of the body and can be pre-computed from a numerical solution of the outer hybrid problem (7.1)–(7.4). In contrast, the matrix M depends on the shape of the body and must be computed from the linear Stokes problem (7.6)–(7.8). For certain cross-sectional shapes, such as an ellipse, $\mathbf{M}$ can be determined analytically. For more general shapes $\mathbf{M}$ can be computed numerically from an application of fast multipole methods to a boundary integral formulation (see §5.1 of [Titcombe *et al.* (2000)] and [Greengard *et al.* (1996)]). This approach was used in [Titcombe *et al.* (2000)] to determine lift and drag coefficients, accurate to all powers of $-1/\log \varepsilon$, for flow past a cylinder of arbitrary cross-section.

The extension of the theory in §4–§6 to determine the drag and lift coefficients for flow past a cylinder of arbitrary cross-section is in principle straightforward. We again have that the far-field behavior of the Stokes solution has the form (7.9), and so the nonlinear algebraic system (7.11) for $\mathbf{S}$ still applies. However, for the nanocylinder problem, M depends on the body shape and on the sliplength l, while for the porous cylinder problem M depends on the body shape and the Darcy number Da. The development of efficient numerical algorithms to compute $\mathbf{R}(\mathbf{S})$ and M are beyond the scope of this paper. However, when these two quantities are available, the numerical solution $\mathbf{S}$ to (7.11) will provide drag and lift coefficients for flow that are accurate to all powers of $-1/\log \varepsilon$.

Acknowledgements

M. J. W. is grateful for the grant support by NSERC (Canada).

Appendix

A. The Drag Coefficient

[Imai (1951)] gives an expression for the drag force in terms of an arbitrary closed circular contour of radius r_0 surrounding the circular cross-section of the cylinder. Converting this expression to polar coordinates, and defining the Reynolds number as $\varepsilon \equiv \mathrm{Re} \equiv U_\infty L \rho_f / \mu$, we can express the drag coefficient, C_D, as

$$\begin{aligned} C_D \;=\; & \frac{r_0}{2} \int_0^{2\pi} \left[\cos\theta \left(\frac{\partial \psi}{\partial r} \right)^2 - \frac{\cos\theta}{r^2} \left(\frac{\partial \psi}{\partial \theta} \right)^2 - \frac{2 \sin\theta}{r} \frac{\partial \psi}{\partial r} \frac{\partial \psi}{\partial \theta} \right] \Bigg|_{r=r_0} d\theta \\ & - r_0 \int_0^{2\pi} (\sin\theta)\, \omega \frac{\partial \psi}{\partial \theta}\Big|_{r=r_0} d\theta + \frac{r_0^2}{\varepsilon} \int_0^{2\pi} (\sin\theta) \frac{\partial \omega}{\partial r}\Big|_{r=r_0} d\theta - \frac{r_0}{\varepsilon} \int_0^{2\pi} (\sin\theta)\, \omega|_{r=r_0}\, d\theta \,. \end{aligned} \tag{A.1}$$

Here ψ satisfies (2.1)–(2.3) and the vorticity ω is $\omega = -\Delta\psi$.

To evaluate the integrals in this expression for C_D when $\varepsilon \to 0$, we use the far-field behavior

$$\psi \sim S \left(r \log r - \frac{r}{2} + \frac{1}{2r} \right) \sin\theta \,, \tag{A.2}$$

valid for $r \to \infty$, of the Stokes solution. By symmetry, only the last two integrals in the expression for C_D are non-zero, and consequently

$$C_D \sim \frac{r_0^2}{\varepsilon}\int_0^{2\pi}(\sin\theta)\,\frac{\partial\omega}{\partial r}\Big|_{r=r_0}\,d\theta - \frac{r_0}{\varepsilon}\int_0^{2\pi}(\sin\theta)\omega|_{r=r_0}\,d\theta\,. \tag{A.3}$$

Since $\omega = -2Sr^{-1}\sin\theta$, (A.3) becomes $C_D \sim 4\pi\varepsilon^{-1}S$, as given in (2.25).

Appendix

B. The Streamfunction for Flow Past a Porous Cylinder

In this appendix we derive (5.1)–(5.6) for the streamfunction for flow past a porous cylinder. Inside the cylinder, we assume that the flow is governed by the Brinkman equation

$$\nabla P^i = -\frac{\mu}{k}\mathbf{v}^i + \hat{\mu}\Delta\mathbf{v}^i\,. \tag{B.1}$$

Here k is the permeability of the porous cylinder, μ is the dynamic viscosity of the fluid, $\hat{\mu}$ is the effective viscosity of the porous medium, P^i is the pressure, and $\mathbf{v^i} = (\mathbf{v_r^i}, \mathbf{v_\theta^i})$ is the fluid velocity in the porous medium. The components of the fluid velocity in terms of streamfunction can be written as $\mathbf{v^i} = (\mathbf{v_r^i}, \mathbf{v_\theta^i}) = (\partial\psi^\mathbf{i}/(\mathbf{r}\partial\theta), -\partial\psi^\mathbf{i}/\partial\mathbf{r})$.

In general, the effective viscosity $\hat{\mu}$ is not expected to be the same as the viscosity of the fluid μ. [Kim & Russel (1985)] obtained the dependency of the effective viscosity and permeability on the solid volume fraction in a porous media by a renormalization of the Stokes equation. They showed that the Brinkman equation is valid in the limit of dilute porous media. In this limit, the effective viscosity $\hat{\mu}$ can be well approximated by the fluid viscosity μ. Hence, in our derivation below, we assume that $\hat{\mu} = \mu$.

We adopt the following scalings for the equation (B.1)

$$\bar{P^i} = \frac{P^i}{\mu U_\infty/L}, \qquad \bar{\mathbf{v}^\mathbf{i}} = \frac{\mathbf{v^i}}{U_\infty}, \qquad \bar{r} = \frac{r}{L}\,.$$

Upon dropping the overbar, we write

$$\nabla P^i = -\chi^2\mathbf{v^i} + \Delta\mathbf{v^i}\,. \tag{B.2}$$

Note that in the case where $\hat{\mu} \neq \mu$, the equation above can be replaced by $1/m\nabla P^i = -(\chi^2/m)\mathbf{v^i} + \Delta\mathbf{v^i}$, where $m = \hat{\mu}/\mu$. Therefore, the scaling, governing equations and boundary conditions will not change. In (B.2), the pressure can be eliminated by taking the curl of the Brinkman equation. Then, we obtain (5.2) upon substituting the velocity components in terms of the streamfunction. Outside the porous cylinder, the flow is governed by (5.1). Modelling the porous medium by the Brinkman equation rather than Darcy's law allows us to satisfy the the continuity of velocity and stresses at the interface between the fluid region and porous cylinder. The validity of the interfacial boundary conditions is discussed in [Vafai & Kim (1995)]. We may write the boundary conditions at the interface as follows:

Continuity of velocity components:

$$v_r^i = v_r^e \Rightarrow \frac{\partial\psi^i}{\partial\theta} = \frac{\partial\psi^e}{\partial\theta} \Rightarrow \psi^i = \psi^e\,, \qquad \text{on} \quad r = 1\,.$$

$$v_\theta^i = v_\theta^e \Rightarrow \frac{\partial\psi^i}{\partial r} = \frac{\partial\psi^e}{\partial r}, \qquad \text{on} \quad r = 1\,.$$

Continuity of the traction:

$$\textit{normal stress balance:} \qquad [\![n.T.n]\!] = 0, \qquad \text{across} \quad r = 1\,.$$

$$\textit{tangential stress balance:} \qquad [\![n.T.t]\!] = 0, \qquad \text{across} \quad r = 1\,.$$

Where $[\![A]\!] = [A]^i - [A]^e$ denotes the jump in A across the surface of the porous cylinder. Here T is the traction tensor, $n = e_r$ and $t = e_\theta$ are the unit normal and tangential vectors to the surface of porous cylinder, respectively. We may write the traction tensor as follows:

$$T = \begin{bmatrix} \tau_{rr} - P & \tau_{r\theta} \\ \tau_{r\theta} & \tau_{\theta\theta} - P \end{bmatrix} = \begin{bmatrix} 2\partial v_r/\partial r - P & r^{-1}\partial v_r/\partial\theta + r\partial/\partial r(v_\theta/r) \\ r^{-1}\partial v_r/\partial\theta + r\partial/\partial r(v_\theta/r) & 2r^{-1}\partial v_\theta/\partial\theta + 2v_r/r - P \end{bmatrix}.$$

Upon writing the tangential and normal stress balance in terms of the streamfunction, we apply the continuity of velocity across the interface $r = 1$ to obtain

$$[\![\tau_{r\theta}]\!] = 0 \Rightarrow [\![-\frac{1}{r^2}\frac{\partial^2\psi}{\partial\theta^2} - \frac{1}{r}\frac{\partial\psi}{\partial r} + \frac{\partial^2\psi}{\partial r^2}]\!] = 0 \Rightarrow [\![\partial^2\psi/\partial r^2]\!] = 0$$

$$[\![\tau_{rr} - P]\!] = 0 \Rightarrow [\![\frac{2}{r^2}\frac{\partial\psi}{\partial\theta} - \frac{2}{r}\frac{\partial^2\psi}{\partial r\partial\theta} - P]\!] = 0 \Rightarrow [\![P]\!] = 0 \Rightarrow [\![\frac{\partial P}{\partial\theta}]\!] = 0\,.$$

Then, upon using the Brinkman and Navier-Stokes equations inside and outside the porous cylinder, we obtain

$$-\frac{1}{r}\frac{\partial P^i}{\partial\theta} = -(\nabla^2 - \chi^2)v^i_\theta = -\frac{1}{r}\frac{\partial}{\partial r}\left(r\frac{\partial v^i_\theta}{\partial r}\right) - \frac{1}{r^2}\frac{\partial^2 v^i_\theta}{\partial\theta^2} - \frac{2}{r^2}\frac{\partial v^i_r}{\partial\theta} + \frac{v^i_\theta}{r^2} + \chi^2 v^i_\theta\,,$$

and

$$-\frac{1}{r}\frac{\partial P^e}{\partial\theta} = -\frac{1}{r}\frac{\partial}{\partial r}\left(r\frac{\partial v^e_\theta}{\partial r}\right) - \frac{1}{r^2}\frac{\partial^2 v^e_\theta}{\partial\theta^2} - \frac{2}{r^2}\frac{\partial v^e_r}{\partial\theta} + \frac{v^e_\theta}{r^2}\,.$$

Upon equating these two expressions, and then applying the continuity of velocity and tangential stress, we obtain that

$$-\frac{1}{r}\frac{\partial}{\partial r}\left(r\frac{\partial v^i_\theta}{\partial r}\right) + \chi^2 v^i_\theta = -\frac{1}{r}\frac{\partial}{\partial r}\left(r\frac{\partial v^e_\theta}{\partial r}\right) \Rightarrow \frac{\partial^3\psi^e}{\partial r^3} - \frac{\partial^3\psi^i}{\partial r^3} = -\chi^2\frac{\partial\psi^i}{\partial r}\,, \qquad \text{on} \quad r = 1\,.$$

This completes the derivation of (5.1)–(5.6).

Appendix

C. The Solution to the Stokes Problem for Flow Past Two Cylinders

In this appendix we outline the derivation of (6.12)–(6.16) using the formulation of [Umemura (1982)]. Let $\mathbf{y} = (y_1, y_2)^t = r(\cos\theta, \sin\theta)$, and introduce the bipolar coordinate system (ξ, η) defined by

$$y_1 = r\cos\theta = \frac{c\sinh\xi}{\cosh\xi - \cos\eta}\,, \qquad y_2 = r\sin\theta = \frac{c\sin\eta}{\cosh\xi - \cos\eta}\,. \tag{C.1}$$

Then lines of constant ξ map to the circles $(y_1 - c\coth\xi)^2 + y_2^2 = c^2\mathrm{csch}^2\xi$. Therefore, if we choose α and c by

$$c\coth\alpha = d/2\,, \qquad c\,\mathrm{csch}\alpha = 1\,, \tag{C.2}$$

so that

$$\alpha = \log\left(\frac{d}{2} + \sqrt{\frac{d^2}{4} - 1}\right)\,, \qquad c = \sqrt{\frac{d^2}{4} - 1}\,, \tag{C.3}$$

it follows that the region $\mathbb{R}^2\backslash D$ in (6.6) maps 1-1 to the rectangle $\Omega \equiv \{(\xi,\eta)\,|\,|\xi|\le\alpha\,,\,-\pi<\eta\le\pi\}$, and that $(\xi,\eta)\to\mathbf{0}$ corresponds to $r\to\infty$. For $r\to\infty$, we readily obtain the following local behavior of the mapping (C.1):

$$\xi^2+\eta^2\sim\frac{4c^2}{r^2}\,,\qquad \xi\sim\frac{2c\cos\theta}{r}\,,\qquad \eta\sim\frac{2c\sin\theta}{r}\,. \tag{C.4}$$

In terms of these bipolar coordinates, (6.6)–(6.9) is transformed to a problem for $\Phi(\xi,\eta)$ given by (cf. [Jeffrey (1922)])

$$[\partial_{\xi\xi\xi\xi}+2\partial_{\xi\xi\eta\eta}+\partial_{\eta\eta\eta\eta}-2\partial_{\xi\xi}+2\partial_{\eta\eta}+1]\,\Phi=0\,,\qquad (\xi,\eta)\in\Omega\,, \tag{C.5}$$

$$\Phi=\Phi_\xi\;=\;0\,,\quad \text{on}\quad \xi=\pm\alpha\,;\qquad \Phi\quad\text{is } 2\pi \text{ periodic in } \eta\,, \tag{C.6}$$

with Φ having an appropriate singularity behavior as $(\xi,\eta)\to\mathbf{0}$. In particular, $\Phi\to 0$ but is not C^1 as $(\xi,\eta)\to\mathbf{0}$. In terms of Φ, the solution ψ_c to (6.6)–(6.9) is

$$\psi_c(y_1,y_2)=\Psi\left[\xi(y_1,y_2),\eta(y_1,y_2)\right]\,,\qquad \text{where}\quad \Psi(\xi,\eta)=f\Phi(\xi,\eta)\,,\quad f\equiv\frac{c}{\cosh\xi-\cos\eta}\,. \tag{C.7}$$

The appropriate singularity behavior of Φ as $(\xi,\eta)\to\mathbf{0}$ must be such that, in terms of polar coordinates, it yields $\Psi\sim r\log r\sin\theta$ as $r\to\infty$. Since $f\sim 2c/(\xi^2+\eta^2)=\mathcal{O}(r^2)$ as $(\xi,\eta)\to\mathbf{0}$, or equivalently as $r\to\infty$, from (C.7), we conclude that Ψ has the required far-field behavior provided that

$$\Phi\to 0\,,\quad \text{as}\quad (\xi,\eta)\to\mathbf{0}\quad\text{with local behavior}\quad \Phi\sim-\frac{1}{2}\eta\log(\xi^2+\eta^2)\,. \tag{C.8}$$

To verify this claim, we calculate for $(\xi,\eta)\to\mathbf{0}$ using (C.4) that

$$\Psi=f\Phi\sim\frac{2c}{\xi^2+\eta^2}\left(-\frac{\eta}{2}\log(\xi^2+\eta^2)\right)\sim\frac{2cr^2}{4c^2}\left(-\frac{1}{2}\frac{2c\sin\theta}{r}\log\left(\frac{4c^2}{r^2}\right)\right)\sim r\log r\sin\theta\,, \tag{C.9}$$

as $r\to\infty$. Therefore, the problem (6.6)–(6.9) is transformed to the problem of finding a solution to (C.5)–(C.6) satisfying the local behavior in (C.8) as $(\xi,\eta)\to\mathbf{0}$.

Next, we construct an exact solution of (C.5) with the local behavior (C.8). To determine such a solution, we recall in terms of polar coordinates that $\Delta^2\left[\frac{r^2}{2}\log r\right]=0$. Upon differentiating with respect to y_2, we obtain that $\Delta^2[y_2\log r+y_2/2]=0$, so that $\Delta^2[y_2\log r]=0$. To convert this exact biharmonic solution having the correct behavior at infinity to bipolar coordinates, we first calculate $\log r$ from (C.1) as

$$\log r=\log\left(\frac{c\left(\sinh^2\xi+\sin^2\eta\right)^{1/2}}{\cosh\xi-\cos\eta}\right)=-\frac{1}{2}\log\left(\cosh\xi-\cos\eta\right)+\frac{1}{2}\log\left(\cosh\xi+\cos\eta\right)+\log c\,. \tag{C.10}$$

Then, upon calculating $y_2\log r$ from using (C.1) for y_2, it follows that an exact solution to (C.5) with the local behavior (C.8) is

$$\tilde{\Phi}_0=-\frac{1}{2}\sin\eta\log\left(\cosh\xi-\cos\eta\right)+\frac{1}{2}\sin\eta\log\left(\cosh\xi+\cos\eta\right)\,. \tag{C.11}$$

We remark that the second term in (C.11) is regular as $(\xi,\eta)\to\mathbf{0}$ but is not C^1 at $(\xi,\eta)=(0,\pm\pi)$. Moreover, by expanding this term in a Fourier sine series in η to generate a separation of variables type solution, it is readily verified that it satisfies (C.5). As such, an exact solution to (C.5), which has the local behavior (C.8) as $(\xi,\eta)\to\mathbf{0}$, but is otherwise smooth in Ω, is simply the first term in (C.11), which we label by

$$\Phi_0\equiv-\frac{1}{2}\sin\eta\log\left(\cosh\xi-\cos\eta\right)\,. \tag{C.12}$$

We then must add to Φ_0 a smooth solution Φ_s, constructed by using separation of variables applied to (C.5), in order to satisfy the boundary conditions in (C.6) at $\xi = \pm\alpha$. Since Φ_0 is even in ξ, we need only choose Φ_s to be an even function of ξ with $\Phi_s = -\Phi_0$ and $\partial_\xi \Phi_s = -\partial_\xi \Phi_0$ on $\xi = \alpha$.

To expand Φ_0 as a Fourier sine series in η, we first define $z = e^{-\xi+i\eta}$ and derive the identity

$$\sum_{m=1}^{\infty} \frac{e^{-m\xi}}{m}\cos(m\eta) = Re\left[\sum_{m=1}^{\infty}\frac{z^m}{m}\right] = -\log|1-z| = \frac{\xi}{2} - \frac{\log 2}{2} - \frac{1}{2}\log\left(\cosh\xi - \cos\eta\right)\,. \tag{C.13}$$

From this identity, and by using trigonometric addition formulas, we obtain for $\xi > 0$ that Φ_0 has the Fourier sine series

$$\begin{aligned}\Phi_0 &= -\frac{\sin\eta}{2}\left[\xi - \log 2 - 2\sum_{m=1}^{\infty}\frac{e^{-m\xi}}{m}\cos(m\eta)\right]\,,\\ &= -\frac{1}{2}\left(\xi - \log 2 + \frac{1}{2}e^{-2\xi}\right)\sin(\eta) + \frac{1}{2}\sum_{k=2}^{\infty}\left(\frac{e^{-(k-1)\xi}}{k-1} - \frac{e^{-(k+1)\xi}}{k+1}\right)\sin(k\eta)\,.\end{aligned} \tag{C.14}$$

Then, since the Fourier sine series separation of variables solution Φ_s for (C.5), which is even in ξ, is a linear combination of $\cosh[(k+1)\xi]\sin(k\eta)$ and $\cosh[(k-1)\xi)]\sin(k\eta)$ for $k \geq 1$, it follows that the solution $\Phi = \Phi_0 + \Phi_s$ to (C.5)–(C.7) with (C.8) has the form

$$\Phi = h_1(\xi)\sin(\eta) + \sum_{k=1}^{\infty} h_k(\xi)\sin(k\eta)\,, \tag{C.15}$$

where

$$h_1(\xi) \equiv -\frac{\xi}{2} + \frac{\ln 2}{2} - \frac{e^{-2\xi}}{4} - \frac{a_1}{2}\cosh(2\xi) - \frac{b_1}{2}\,, \tag{C.16}$$

$$h_k(\xi) \equiv \frac{1}{2}\left(\frac{e^{-(k-1)\xi}}{k-1} - \frac{e^{-(k+1)\xi}}{k+1}\right) - \frac{a_k}{2}\cosh[(k+1)\xi] - \frac{b_k}{2}\cosh[(k-1)\xi]\,, \quad k \geq 2\,. \tag{C.17}$$

Upon setting $h_k = h_k' = 0$ at $\xi = \alpha$ for $k \geq 1$, we obtain that a_k and b_k for $k \geq 1$ satisfy the linear system

$$a_1\cosh(2\xi) + b_1 = -\alpha + \ln 2 - \frac{1}{2}e^{-2\alpha}\,, \qquad 2a_1\sinh(2\alpha) = -1 + e^{-2\alpha}\,, \tag{C.18}$$

$$a_k\cosh\left[(k+1)\alpha\right] + b_k\cosh\left[(k-1)\alpha\right] = \frac{e^{-(k-1)\alpha}}{k-1} - \frac{e^{-(k+1)\alpha}}{k+1}\,, \qquad k \geq 2\,, \tag{C.19}$$

$$a_k(k+1)\sinh\left[(k+1)\alpha\right] + b_k(k-1)\sinh\left[(k-1)\alpha\right] = e^{-(k+1)\alpha} - e^{-(k-1)\alpha}\,, \qquad k \geq 2\,. \tag{C.20}$$

The solution of this system is given in (6.12)–(6.16).

Finally, we calculate the correction to the local behavior of Φ as $(\xi,\eta) \to \mathbf{0}$. We obtain from (C.15)–(C.17) that

$$\Phi \sim -\frac{\eta}{2}\log\left(\frac{\xi^2+\eta^2}{2}\right) - \frac{\eta}{2}\sum_{m=1}^{\infty} m(a_m + b_m) \quad \text{as} \quad (\xi,\eta) \to \mathbf{0}\,. \tag{C.21}$$

Recalling that $\Psi = f\Phi$, we use the local behavior (C.4) to obtain that ψ_c has the form (6.9) where q is defined in (6.12). This completes the derivation of (6.12)–(6.16).

References

Chen & Ward (2011). Chen, W., & Ward, M.J. 2011 The stability and dynamics of localized spot patterns in the two-dimensional Gray-Scott model, *SIAM J. Appl. Dyn. Sys.*, **10**(2) 582–666.

Dorrepaal §O'Neil (1979). Dorrepaal J.M., & O'Neil, M.E. 1979 The existence of free eddies in a streaming Stokes flow, *Q. J. Mech. Appl. Math.,* **32**, 95–107.

Greengard *et al.* (1996). Greengard, L., Kropinski, M.C., & Mayo A. 1996 Integral equation methods for Stokes flow and isotropic elasticity in the plane, *J. Comput. Physics,* **125**(2), 403–414.

Hinch (1991). Hinch, J. 1991, Perturbation methods, *Cambridge Texts in Applied Mathematics, Cambridge U. Press, Cambridge U.K.*

Imai (1951). Imai, I. 1951 On the asymptotic behaviour of viscous fluid flow at a great distance from a cylindrical body, with special reference to Filon's paradox, *Proc. Roy. Soc. A.,* **208**, 487–516.

Jeffrey (1922). Jeffrey, G.B. 1922 The rotation of two circular cylinders in a viscous fluid, *Proc. Roy. Soc. A*, **101**, 169–174.

Kaplun (1957). Kaplun, S. 1957 Low Reynolds number flow past a circular cylinder, *J. Math. Mech.,* **6**(5), 52–60.

Keller & Ward (1996). Keller, J.B., & Ward, M.J. 1996 Asymptotics beyond all orders for a low Reynolds number flow, *J. Eng Math.,* **30**, 253–265.

Kevorkian & Cole (1996). Kevorkian, J., & Cole, J. 1996 Multiple scale and singular perturbation methods, *Applied Mathematical Sciences Vol. 114, Springer, New York*

Kim & Russel (1985). Kim, S., & Russel, W.B. 1985 Modelling of porous media by renormalization of the Stokes equations, *J. Fluid Mech.,* **154**, 269–286.

Kohr *et al.* (2009). Kohr, M., Prakash, J., Sekhar, G.P.R., & Wendland, W.L. 2009 Expansions at small Reynolds numbers for the flow past a porous circular cylinder, *Applicable Analysis,* **88**(7), 1093–1114.

Kolokolnikov *et al.* (2005). Kolokolnikov, T., Titcombe, M., & Ward, M.J. 2005 Optimizing the fundamental Neumann eigenvalue for the laplacian in a domain with small traps, *European J. Appl. Math.,* **16**(2) 161–200.

Kropinski *et al.* (1995). Kropinski, M.C., Ward, M.J., & Keller, J.B. 1995 A hybrid asymptotic-numerical method for low Reynolds number flows past a cylindrical body, *SIAM J. Appl. Math.,* **55**(6), 1484–1510.

Kropinski *et al.* (2011). Kropinski, M.C., Lindsay, A., & Ward, M.J. 2011 Asymptotic analysis of localized solutions to some linear and nonlinear biharmonic eigenvalue problems, *Studies Appl. Math.,* **126**(4), 347–408.

Lagerstrom (1988). Lagerstrom, P.A. 1988 Matched Asymptotic Expansions, *Applied Mathematical Sciences Vol. 76, Springer-Verlag, New York.*

Lee & Leal (1986). Lee, S.H., & Leal, L.G. 1986 Low Reynolds number flow past cylindrical bodies of arbitrary cross-sectional shape, *J. Fluid Mech.,* **164**, 401–427.

Matthews & Hill (2006). Matthews, M.T, & Hill, J.M. 2006 Flow around nanospheres and nanocylinders, *Quarterly J. Mechanics Appl Math.,* **59**(2), 191–210.

Miyazaki & Hasimoto (1980). Miyazaki, T., & Hasimoto, H. 1980 Separation of creeping flow past two circular cylinders, *J. Phys. Soc. of Japan,* **49**(4), 1611-1618.

Navier (1823). Navier, C.L.M.H 1823 Mémoire sur les lois du mouvement des fluides, *Mémoire de l'Académie Royale des Sciences de l'Institut de France*, 389–440.

O'Malley (2010). O'Malley, R.E. 2010 Singular perturbation theory: A viscous flow out of Göttingen, *Annu Rev. Fluid Mech.,* **42**, 1–17.

Pillay *et al.* (2010). Pillay, S., Ward, M.J, Pierce, A., Kolokolnikov, T. 2010 An asymptotic analysis of the mean first passage time for narrow escape problems: Part I: two-dimensional domains, *SIAM Multiscale Mod. and Sim.,* **8**(3), 803–835.

Proudman & Pearson (1957). Proudman, I., & Pearson, J. 1957 Expansions at small Reynolds number for the flow past a sphere and a circular cylinder, *J. Fluid Mech.,* **2**, 237–262.

Ranger (1995). Ranger, K.B. 1995 Explicit solutions of the steady two-dimensional Navier-Stokes equations, *Studies Appl. Math.,* **94**(2), 169–181.

Sen *et al.* (2009). Sen, S., Mittal, S., & Biswas, G. 2009 Steady separated flow past a circular cylinder at low Reynolds numbers, *J. Fluid Mech.,* **620**, 89-119.

Skinner (1975). Skinner, L.A. 1973 Generalized expansions for slow flow past a cylinder, *Q. J. Mech. Appl. Mech.,* **28**(3), 333-340.

Titcombe *et al.* (2000). Titcombe, M., Ward, M.J., & Kropinski M.C. 2000 A hybrid asymptotic-numerical solution for low Reynolds number flow past an asymmetric cylindrical body, *Studies Appl. Math.,* **105**(2), 165–190.

Tritton (1959). Tritton, D.J. 1959 Experiments on the flow past a circular cylinder at low Reynolds numbers, *J. Fluid Mech.,* **6**, 547–567.

Umemura (1982). Umemura, A. 1982 Matched-asymptotic analysis of low-Reynolds-number flow past two equal circular cylinders, *J. Fluid Mech.,* **121**, 345–363.

Vafai & Kim (1995). Vafai, K. & Kim, S.J. 1995 On the limitations of the Brinkman-Forchheimer-extended Darcy equation, *Int. J. Heat and Fluid Flow,* **16**, 11–15.

Van Dyke (1975). Van Dyke, M. 1975, Perturbation methods in fluid mechanics, *Parabolic Press, Stanford, Palo Alto.*

Veysey & Goldenfeld (2007). Veysey II, J. & Goldenfeld, N. 2007 Simple viscous flows: from boundary layers to the renormalization group, *Reviews of Modern Physics,* **79**, 883–927.

Ward & Kropinski (2010). Ward, M.J., & Kropinski, M.C. 2010 Asymptotic methods for PDE problems in fluid mechanics and related systems with strong localized perturbations in two dimensional domains, *book chapter in: Asymptotic Methods in Fluid Mechanics: Surveys and Results. CISM International centre for mechanical science,* **523**, 23–70.

Ward *et al.* (1993). Ward, M.J., Henshaw, W.D.. & Keller, J.B. 1993 Summing logarithmic expansions for singularly prturbed eigenvalue problems, *SIAM J. Appl. Math.*, **53**(3) 799–828.